Whiterocks Mountain Alkaline Complex, South-Central British Columbia: Geology and Platinum-Group-Element Mineralization

By Graham T. Nixon and Brent Carbno

KEYWORDS: Platinum-group-elements, Whiterocks Mountain, alkaline complex, sulfides, mineralogy, electron-microprobe analysis.

INTRODUCTION

The recent increase in the price of platinum-group elements (PGE) in world markets has sparked renewed interest in exploration for these metals. Although world-class deposits of PGE such as those associated with tholeiitic or komatiitic flood-basalt provinces (*e.g.* Noril'sk–Talnakh, Russia, and Kambalda, Western Australia) and large layered intrusions (*e.g.* Bushveld, South Africa) have yet to be discovered in the Cordillera, there are other prospective geological environments specific to the supra-subduction zone setting which characterizes much of Cordilleran evolution. For example, placer and lode occurrences associated with Alaskan-type ultramafic-mafic intrusive complexes are known to host PGE as a primary commodity (*e.g.* Tulameen, southern British Columbia, *cf.* Nixon *et al.*, 1997 for a summary relevant to British Columbia). In addition, there are other predominantly sulfide-bearing environments where the PGE occur as a subsidiary component of certain base- and precious-metal (Cu±Au±Ag) deposit types which are common in the Cordillera such as porphyry environments (*e.g.* Copper Mountain-Ingerbelle) and Cu-PGE (±Au±Ag) mineralization associated with alkalic intrusive complexes (*e.g.* Maple Leaf showing in the Franklin Camp (Averill Complex); and the Sappho prospect, southern British Columbia). The latter style of mineralization has been informally referred to as "Coryell-type" after the alkaline rocks of the Tertiary (Eocene) Coryell Batholith in southern British Columbia (Hurlbert *et al.* 1988). Clearly, given current metal prices, even the typically low tenor of PGE in these latter deposit types has the potential to attract exploitation of an otherwise subeconomic base- and precious-metal resource.

In an effort to promote further exploration for PGE in British Columbia, a new mapping and sampling program was undertaken to examine PGE-bearing sulfide environments in the Cordillera. Fieldwork this past summer focused on the Whiterocks Mountain alkaline intrusive complex in south-central British Columbia where previous work by industry has revealed anomalous concentrations of PGE associated with Cu-Fe sulfides in a "Coryell-type" intrusive setting. The results of recent geological mapping together with lithogeochemical and mineral analyses are reported below. In addition, a companion contribution (Dunn *et al.*, this volume) presents preliminary results for a soil survey employing new techniques which are capable of detecting Pt at ultra-low concentrations (~0.1 ppb).

LOCATION AND ACCESS

The Whiterocks Mountain alkaline plutonic complex is named for Whiterocks Mountain (50.01°N, 119.75°W; 1873 m) which is situated west of Okanagan Lake approximately 25 kilometres northwest of Kelowna (Figure 1). The map area straddles the boundary between two 50 000-scale topographic sheets (NTS 82L/4 and 82E/13)

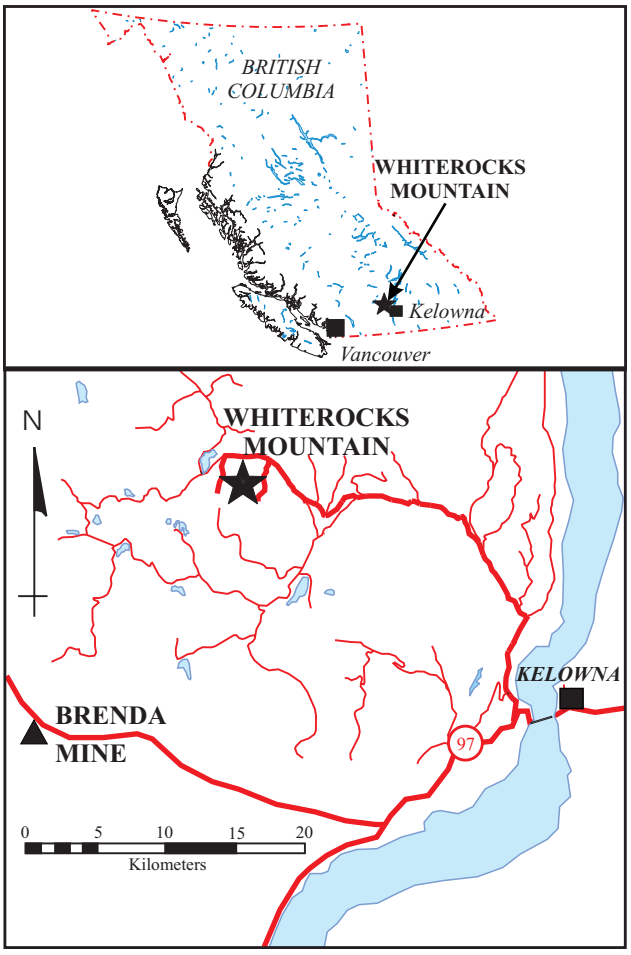

Figure 1. Location of the Whiterocks Mountain area, south-central British Columbia.

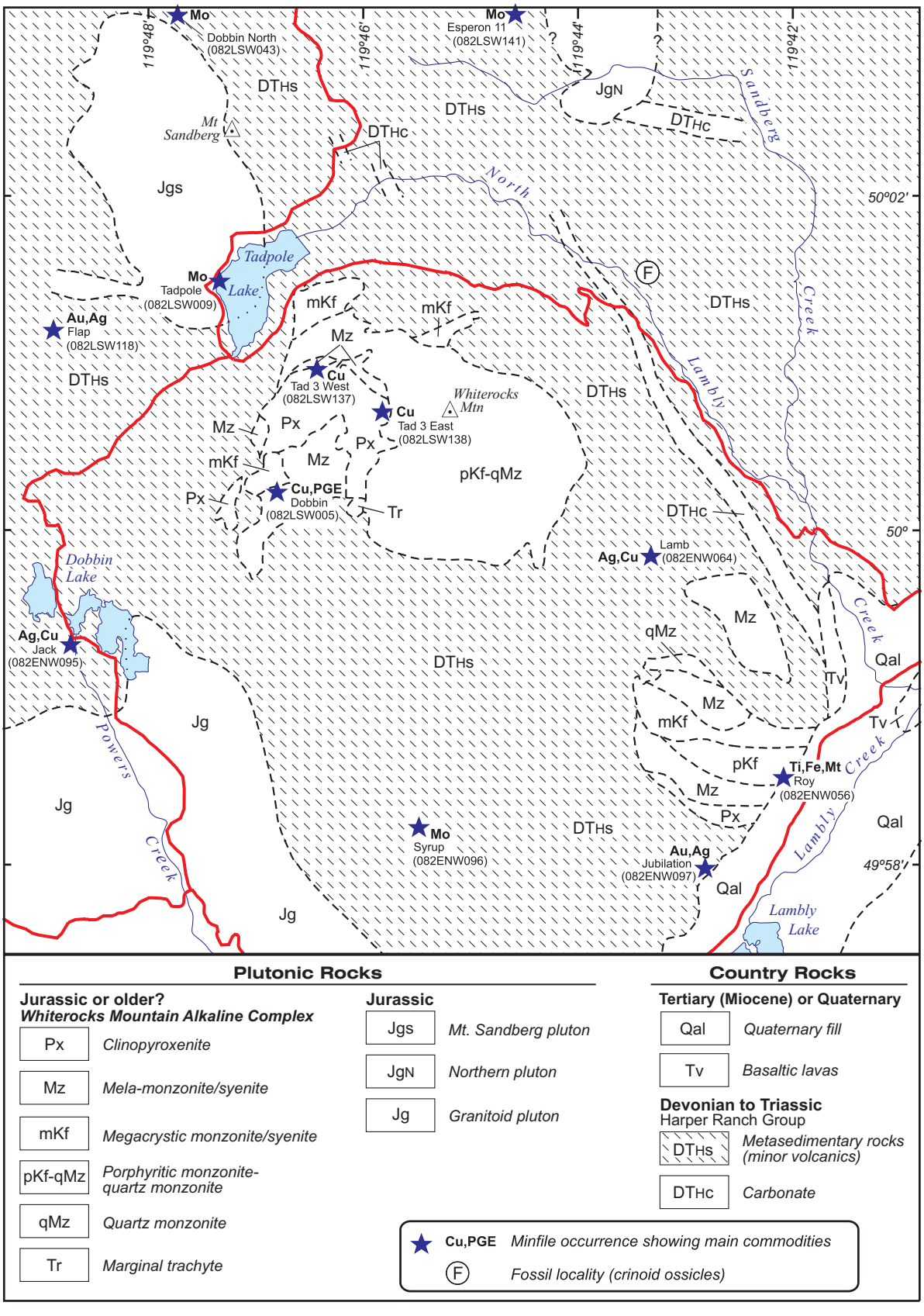

Figure 2. Generalized geological map of the Whiterocks Mountain area showing MINFILE occurrences. The star for the Dobbin Cu-PGE prospect marks the location of the 1997 drill program referred to in the text.

near the eastern margin of the Thompson Plateau. Road access is via the Bear Main Forest Services road which leaves West Okanagan Lake Road on the west shore of Okanagan Lake just north of Bear Creek Provincial Park. The Whiterocks Main logging road leaves Bear Main at Kilometre 17 for the Tadpole Lake area where a system of spur roads maintained by Riverside Forest Products of Kelowna provide excellent access to the map area. The hilly topography is well forested with pine and spruce and generally covered by a thin veneer of glacial drift.

MINERAL OCCURRENCES AND EXPLORATION HISTORY

The MINFILE occurrences for base- and precious-metals in the region are numerous. The most notable is the former Brenda Mine which is located about 24 kilometres southwest of Whiterocks Mountain (Figure 1). This Cu-Mo porphyry deposit produced approximately 272 000 tonnes of copper, 65 000 tonnes of molybdenum, 113 000 kg of silver and 1800 kg of gold over its 20-year mine life (1970-1990; Weeks *et al.* 1995). Figure 2 shows the MINFILE occurrences in the project area. The two principal prospects in the vicinity of Whiterocks Mountain are the Dobbin Cu-Pd-Pt (MINFILE 082LSW005) and Tadpole Mo (082LSW009) occurrences. The main (Dobbin) copper anomaly in the area was named for Dobbin Lake. The Tadpole Mo showing, located on the west shore of Tadpole Lake, is partially submerged beneath the waters of the enlarged reservoir. The Dobbin and Tadpole showings are currently covered by claims owned by joint venture partners Verdstone Gold Corporation and Molycor Gold Corporation.

The first prospectors to enter the area arrived at the beginning of the 20th century or earlier. Intermittent exploration activity ensued until the late 1960s and early 1970s when a succession of exploration companies following copper and molydenum stream-silt anomalies in the area around Whiterocks Mountain performed considerable work involving geological mapping, trenching, soil and rock-chip geochemistry, magnetometer and induced-polarization surveys, and percussion and diamond drilling (details are given in the British Columbia Ministry of Energy and Mines Assessment Reports). It was this work that established and first tested the molybdenum anomaly at Tadpole Lake and the main copper anomaly at the Dobbin property. Grades encountered in drilling ranged 0.1-0.4 % Cu and up to 0.017 % Mo with Ag ~3.4 g/t over intersections of up to 44.8 m.

Following this activity, Cominco Limited acquired the ground in 1977 and through to 1980 performed extensive work which further delineated mineralization, produced detailed geological maps and supported an M.Sc. thesis (Osatenko, 1978, 1979a, 1979b, 1980; Mehner, 1982). According to this work, mineralization at the Tadpole showing is related to a porphyry Mo system with the most intense mineralization centered on a quartz stockwork zone (1.5 x 1 km) which is focused at the southwestern margin of the granitoid stock. The best drill intersection gave 0.061 % Mo over 180 ft. Rock-chip samples collected at the main Dobbin copper anomaly yielded grades similar to previous results (0.014-0.017 % Mo; 0.2-0.4 % Cu). During the course of this work, Cominco geologists apparently were the first to analyze for PGE. Rock chip samples from the main copper anomaly returned maximum abundances of 390 ppb Pt and 265 ppb Pd (fire assay) combined with low Au and Ag (40 ppb and 2 ppm, respectively). It was noted that the PGE appear to be preferentially associated with disseminated sulfides (pyrite-chalcopyrite-bornite) in hornblende pyroxenites of the Whiterocks Mountain complex and cross-cutting epidote-albite veins, and the style of mineralization was related to an alkaline porphyry deposit type.

Almost a decade later, Chevron Canada Resources Ltd. conducted several prospecting surveys on the northwest flank of Whiterocks Mountain about 1.5 kilometres northeast of the main Dobbin copper anomaly (MINFILE 082LSW137). Soil and rock-chip samples indicated anomalous metal concentrations of ~2000 ppm Cu, 240 ppb Pt, 80 ppb Pd and 29 ppb Au.

In 1997, Verdstone/Molycor, the current owners of the Dobbin property, conducted soil and lithogeochemical sampling of the "central" (main) Dobbin copper anomaly, and 22 diamond drill holes (4689 m) were completed and logged. The best drill intersection yielded 0.19 % Cu, 0.41 g/t Pt and 0.35 g/t Pd over 111 m (288-399 m depth), which includes a 15 m zone of 0.54 % Cu, 1.32 g/t Pt and 0.95 g/t Pd (333-348 m; Makepeace, 2000). The core from this intersection was resampled and analyzed during the course of this study. The new results confirm the anomalously high concentrations of PGE in the core (discussed below).

PREVIOUS WORK AND REGIONAL GEOLOGY

The map area straddles the boundary (50° N) between original 250 000-scale mapping done by the Geological Survey of Canada. The northern part of the area lies within the Vernon sheet (Jones, 1959) and the southern portion is covered by the Kettle River west half sheet (Cairnes, 1940; Little, 1961). A 250 000-scale compilation of the Thompson-Shushwap-Okanagan region by Okulitch (1979) covers the entire Whiterocks Mountain area and draws heavily on previous mapping (Okulitch, personal communication, 2000); and Okulitch (1989) subsequently published a revision of parts of the geology. A compilation by Templeman-Kluit (1989) at the same scale covers the southern part of the map area. In addition, both the Vernon and Penticton (NTS 82E) sheets were re-compiled at 250 000-scale during the Provincial Mineral Potential Project .

The Whiterocks Mountain alkaline complex was the subject of a M.Sc. thesis by Mehner (1982) who produced a geological map (5000-scale) and the first detailed petrographic and geochemical descriptions. Although details differ, his geology is basically the same as the Cominco property map provided by Osatenko (1979a)

who also produced a detailed map of the stock west of Tadpole Lake.

In terms of its regional stratigraphic setting, the Whiterocks Mountain area lies near the eastern margin of the Intermontane Belt within the Quesnellia tectonostratigraphic terrane (Harper Ranch subterrane). The oldest rocks in the region belong to the Paleozoic Chapperon Group which lies just outside the map area to the west and north. Ultramafic bodies within the Chapperon Group, known as the Old Dave "intrusions", are probably remnants of an obducted sliver of oceanic crust presumably emplaced within a Paleozoic subduction complex off to the west. The hostrocks of the Whiterocks Mountain alkaline complex comprise a series of deformed and metamorphosed, Paleozoic volcanic and sedimentary rocks including limestone, argillite, chert and conglomerate (Figure 2). In the most recent compilation (Provincial Mineral Potential Project), these rocks have been assigned to the Devonian to Triassic Harper Ranch Group. The youngest stratigraphic units in the surrounding region include Tertiary (Eocene) volcanic flows and sedimentary sequences of the Kamloops Group, basaltic lavas of the Chilcotin Group (Miocene and younger) and Quaternary valley basalt. Plutonism in the vicinity of the map area, including the Whiterocks Mountain complex, has been assigned to the Late Jurassic (Okulitch, 1989). The region as a whole has been subjected to a Tertiary (Eocene) extensional and thermal event which occurred contemporaneous with the emplacement of alkalic plutons of the Coryell Suite.

WHITEROCKS MOUNTAIN ALKALINE COMPLEX

The Whiterocks Mountain stock was originally subdivided by Osatenko and Mehner into a quartz-deficient alkalic complex underlying Whiterocks Mountain, which is the focus of this study, and a quartz-enriched calc-alkaline complex extending north-northwesterly from Tadpole Lake, referenced herein as the Mt. Sandberg pluton (Figure 2). Based on their contrasting petrography, geochemistry and styles of mineralization, both authors considered the alkaline and calc-alkaline complexes to be genetically unrelated. The contact between these intrusive bodies is not exposed and they appear to be separated by a screen of country rock about 700m wide at surface. In this report, the Mt. Sandberg pluton is treated as a completely separate entity and is considered to be genetically distinct from the alkaline stock at Whiterocks Mountain.

The age of the Whiterocks Mountain alkaline complex (Whiterocks complex) is poorly determined. Biotite mineral separates from a biotite clinopyroxenite have yielded a two-point Rb-Sr isochron age of 149 ± 22 Ma (R. L.Armstrong *in* Mehner, 1982). Whole-rock plus mineral isochrons (biotite, hornblende, and potassium feldspar separates) for a porphyritic monzonite and leucocratic quartz monzonite have produced Rb-Sr isochron ages of 291 ± 38 Ma and 338 ± 37 Ma, respectively (Wilkins, 1981). On the other hand, conventional K-Ar dating of porphyritic monzonite and hornblende clinopyroxenite gave isotopic ages of 169 ± 6 Ma and 174 ± 6 Ma (Wilkins, 1981). In addition, calc-alkaline quartz diorite dikes which cut the alkaline rocks have yielded K-Ar dates of 147 ± 5 Ma and 145 ± 5 Ma, and a concordant Rb-Sr isochron age of 154 ± 6 Ma. Taken as a whole, these data indicate that the alkaline complex is Mesozoic or Paleozoic in age, and evidently much too old to be correlative with Eocene alkaline rocks of the Coryell batholith.

As previously mapped, the Whiterocks complex occupied an area of about 9 km^2 and its contact east of Whiterocks Mountain was poorly defined. New mapping on recently constructed logging roads has better delineated the eastern contact and recognized a sizeable (~4 km^2) extension of the complex to the southeast near Lambly Creek. An area of sparse outcrop (1.5 km in width), which represents a relatively thin carapace of country rock, divides the Whiterocks Mountain stock into a northern and southern cupola. The northern cupola occupies a subcircular outcrop area of approximately 3.5 km maximum diameter centered just west of Whiterocks Mountain. The mafic and ultramafic rocks are restricted to the western half of the stock and have a north-northeasterly distribution. The more leucocratic, quartz-bearing monzonites forming the eastern half of the intrusion have a northwesterly elongation and at their northern extremity transect the melanocratic rocks. The southern cupola comprises a northwesterly trending intrusion at least 2 kilometres in length which disappears to the southeast beneath thick Quaternary alluvial deposits occupying the Lambly Creek drainage. A smaller satellitic body of monzonite crops out 300 m beyond the northeastern contact with the country rocks. As discussed below, the southern cupola embodies all of the major rocks types found to the north and is similarly characterized by a well-defined high on the aeromagnetic map (Geological Survey of Canada, 1968). Interestingly, this body is also coincident with a Ti-Fe (-magnetite) occurrence in the MINFILE database (Figure 2).

The principal rock types of the Whiterocks complex comprise a diverse suite of porphyritic to non-porphyritic ultramafic, mafic and felsic plutonic rocks and related minor intrusions. The map units shown in Figure 2 essentially correspond to lithologies identified by Mehner (1982). They include biotite- and hornblende-bearing clinopyroxenites and their feldspar-bearing variants, clinopyroxene- and hornblende-bearing melanocratic monzonites and syenites, porphyritic and megacrystic monzonites and syenites with conspicuously large crystals of potassium feldspar, and leucocratic quartz monzonites; minor lithologies include hornblendite and hornblende gabbro/diorite, leuco-syenite and rare trachyte.

Many of the rocks exhibit textures which may be described in terms of classical cumulate terminology. This does not necessarily imply that these lithologies were formed by gravitative settling of crystals, although this is considered as a likely concentration mechanism for the

crystal cumulates which form the clinopyroxenites and hornblende gabbro/diorites.

The mineralogical descriptions which follow make frequent reference to "biotite" and "hornblende" ; these terms are used a generic sense to indicate ferromagnesian mica and calcic amphibole, respectively. Electron-microprobe analyses of these minerals allow for a more specific nomenclature which is discussed below. Although quartz appears in the more leucocratic rocks, feldspathoids appear to be completely lacking. Of note, however, is the presence of igneous garnet in a number of monzonitic samples.

Clinopyroxenite and Hornblendite

The best exposures of the ultramafic lithologies are found due west of Whiterocks Mountain summit. Dark greenish grey to almost black, medium-grained clinopyroxenites generally contain both hornblende and biotite in variable proportions, accessory magnetite and apatite, and may carry small amounts of disseminated sulfide. Locally, hornblende forms large (≤3 cm) poikilitic crystals enclosing pyroxene. Outcrops are strongly magnetic and commonly cut by planar veins of hornblendite or hornblende+feldspar (partially epidotized) from several millimetres to centimetres in width. Anastomizing, virtually monomineralic veins and irregular clots of coarse-grained to pegmatitic biotite crystals (5 mm to 2 cm) are a conspicuous feature of many outcrops, although not nearly as prevalent as the hornblendite veins. Clinopyroxenites and hornblendites with subequal proportions of amphibole and pyroxene occur on the margins of the mappable clinopyroxenite bodies near contacts with melanocratic monzonite-syenite. They commonly contain small amounts of feldspar and are observed to grade over narrow intervals into gabbro/diorite and melanocratic monzonite.

In thin section, subhedral to anhedral, colourless to very pale green and weakly pleochroic clinopyroxenes (≤5 mm) have cumulus textures and may exhibit rare schillered features and a weak preferred orientation. Some clinopyroxenites contain oscillatory zoned, and rarely, sector zoned crystals. Inclusions of euhedral biotite, magnetite and apatite have been observed but not primary amphibole. Pyroxenes in hornblende-bearing rocks are usually flecked with patchy to vermicular amphibole whose optical properties are similar to the igneous amphiboles and quite distinct from secondary, uralitic green amphibole which partially replaces some grains. Euhedral to anhedral, cumulus to intercumulus biotite, (≤3 mm) is strongly pleochroic from colourless to reddish brown or very dark brown and locally exhibits incipient bleaching (green biotite) and chloritic alteration. Inclusions of biotite have been observed in pyroxene and hornblende, and in some rocks, exsolution of acicular rutile, probably caused by subsolidus oxidation, has produced a sagenitic texture. Anhedral, intercumulus poikilitic hornblende (typically ≤5 mm) shows olive-green to dark green or brown pleochroism and is locally altered to secondary actinolitic amphibole. In the more hornblende-rich clinopyroxenites, amphibole joins pyroxene as a cumulus phase. Euhedral to anhedral magnetite (≤0.5 mm) and apatite (≤1.3 mm) occur as ubiquitous cumulus and intercumulus grains whose modal abundances reach about 8 and 4 vol. %, respectively. In particular, apatite locally forms disrupted monomineralic cumulate layers several millimetres thick and over a centimetre in length. Anhedral, patchy zoned plagioclase partially altered to sericite, epidote and clay minerals forms a minor (trace to 5 vol. %) intercumulus phase in feldspathic clinopyroxenites and hornblendites. The feldspathic hornblendites may also contain trace amounts of subhedral to anhedral brownish sphene as an intercumulus phase. In addition, disseminations and veins of sulfides, predominantly pyrite and chalcopyrite, occur as trace or minor constituents and are discussed further below in reference to the mineralization.

Melanocratic Monzonite-Syenite

Scattered outcrops of melanocratic monzonite-syenite (mela-monzonite) are found in the northern cupola north and south of the main pyroxenite body, and in the southern cupola, along the northern margin of the clinopyroxenite as well as further north (Figure 2). Medium grey-brown to greenish brown-weathering, mela-monzonites contain essential plagioclase and potassium feldspar, as well as hornblende and typically clinopyroxene, and accessory magnetite, apatite and sphene; other minor phases include garnet and biotite. In addition, one fine-grained, more leucocratic specimen collected at the contact of this map unit with metasedimentary country rocks contains minor quartz (~4 vol. %). In general, the mela-monzonites are equigranular, medium- to coarse-grained rocks with plagioclase:potassium feldspar ratios in the range 3:2 to 1:3 and modal proportions of mafic minerals averaging 20-40 vol. % (Mehner, 1982). Modal layering is commonly observed near contacts with clinopyroxenites. Locally, the layering exhibits a well-defined igneous lamination marked by a preferred orientation of prismatic hornblende crystals (≤1.5 cm) and tabular feldspars (usually potassium feldspar ≤3 cm). Some outcrops exhibit intercalated layers of feldspathic clinopyroxenite and rounded xenoliths of biotite-hornblende clinopyroxenite. Locally, the mela-monzonites are cut by an irregular network of leucocratic feldspathic dikes (≤10 cm in width) and veins of feldspathic hornblendite and hornblende gabbro/diorite. Rusty-weathering outcrops betray the presence of minor amounts of disseminated sulfides.

In thin section, textures range from equigranular to pseudoporphyritic, and the majority of mela-monzonites exhibit a pronounced igneous lamination. The rocks are usually only weakly altered to epidote, sericite, carbonate and clay minerals. Sodic plagioclase (≤5 mm) occurs as subequant to prismatic, subhedral crystals with cumulate textures and commonly displays patchy-zoned cores and oscillatory-zoned mantles. Colourless to very pale

brownish green clinopyroxene (≤3 mm) forms anhedral to subhedral grains, many of which have reacted to form hornblende or occur as relicts enclosed in amphibole. Clinopyroxene-rich mela-monzonites contain subhedral cumulate pyroxene. Brownish green to dark brown hornblende (≤5 mm) generally occurs as anhedral grains poikilitically enclosing feldspar, clinopyroxene, magnetite and apatite through adcumulus growth. Some rocks, however, also contain subhedral cumulus hornblende. Potassium feldspar typically occurs as anhedral interstitial grains or, more rarely, subhedral prismatic crystals. Euhedral microcline with well-developed tartan twinning is found in the porphyritic variants. Pale pinkish brown garnet generally occurs as anhedral poikilitic crystals partially to completely enclosing plagioclase, microcline, clinopyroxene, hornblende and apatite, textures which indicate a magmatic origin. Some grains exhibit a weak colour zoning, and in one sample submitted for electron-probe microanalysis (discussed below) birefringent garnets display fine oscillatory zoning. Euhedral to subhedral apatite, magnetite and pale brownish sphene are ubiquitous accessory phases (trace to 1 vol. %).

Megacrystic Monzonite-Syenite

Excellent exposures of megacrystic monzonite-syenite (megacrystic monzonites) are found in a logging slash at the western extremity of the northern cupola just north of the main Dobbin copper anomaly. Locally, outcrops are stained with hematite and limonite and carry traces of sulfides. The buff-weathering monzonites contain megacrysts of pale grey potassium feldspar (>2.5<15 cm and typically 3-6 cm) set in a medium-grained melanocratic feldspathic groundmass averaging about 25-30 vol. % mafic minerals. Megacryst habits vary from blocky (*e.g.* 5 x 5 cm) to subequant (*e.g.* 12 x 5 cm) to tabular (*e.g.* 10 x 2.5 cm) and typically exhibit a strong trachytic texture (Photo 1). The distribution of megacrysts is non-uniform such that crowded megacryst zones pass gradationally into zones with relatively few megacrysts, and locally, the larger crystals occur in disoriented aggregates. Rare modal layering is defined by thin (<5 mm) laminae of hornblende crystals oriented parallel to the megacryst fabric and traceable for up to 5 metres over the outcrop (Photo 2). The northern megacrystic monzonites are cut by thin (≤10 cm) dikes of feldspathic hornblende clinopyroxenite. Some of these dikes have curvilinear margins and taper out along strike indicating that the host was hot and plastic at the time of intrusion. Sporadic clinopyroxenite or mela-monzonite xenoliths (≤10 cm) with irregular shapes may represent early remobilized dikes. Megacrystic monzonites in the southern cupola are cut by mela-monzonite dikes with pseudoporphyritic textures involving hornblende, clinopyroxene and plagioclase.

Mineralogical differences exist between megacrystic monzonites in the northern cupola, which contain clinopyroxene and hornblende, and those in the southern cupola which carry only biotite. In thin section, the rocks

Photo 1. Microcline-megacrystic monzonite-syenite exhibiting a well-developed igneous flow lamination, western margin of northern cupola, Whiterocks complex. (Knife is 25 cm in length.)

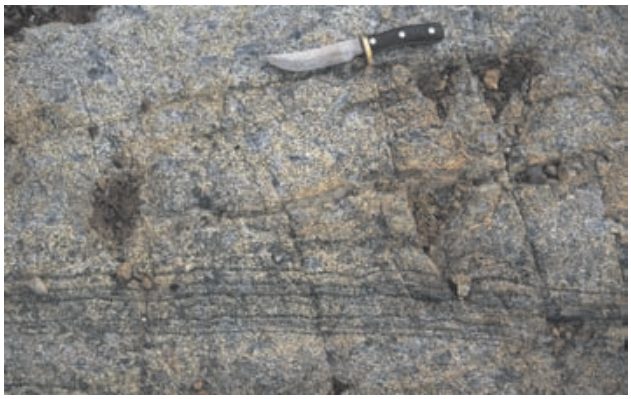

Photo 2. Delicate, hornblende-rich layering (lower part of photograph) in microcline-megacrystic monzonite-syenite, western margin of northern cupola, Whiterocks complex. (Knife is 25 cm in length.)

exhibit weak to moderate alteration to sericite, clay minerals and minor epidote. Microcline megacrysts exhibit distinctive cross-hatched twinning and patchy perthite development, and may contain zonally-arranged inclusions of plagioclase and very fine-scale oscillatory zoning. The northern megacrystic monzonites are more melanocratic with about 30 vol. % mafic minerals in the groundmass. Pale brown to deep olive-green hornblende (≤2 mm) forms subequant to prismatic crystals in a fine- to medium-grained groundmass. Subhedral to anhedral, very pale green clinopyroxene (≤1 mm) has reacted with the melt to form hornblende. Accessory phases, predominantly apatite and magnetite, form up to 1-2 vol. % of the rock. The southern, more leucocratic counterparts contain pale brown to almost black pleochroic biotite (≤1.5 mm; ~15 vol. %) as an interstitial, late-crystallizing phase, and magnetite and apatite in trace amounts.

Porphyritic Monzonite and Quartz Monzonite

Porphyritic monzonites with potassium-feldspar crystals generally measuring 1-2 centimetres in length, and rarely 3-5 centimetres, are found as minor lithologies associated with the main melanocratic monzonite-syenite unit in the southwestern part of the northern cupola, and form a small body in the central part of the southern cupola (Figure 2). In addition, this rock type forms the western part of the composite porphyritic monzonite-quartz monzonite unit underlying the summit region of Whiterocks Mountain and passes into more leucocratic, quartz-bearing lithologies to the east. Mehner (1982) included these quartz-bearing monzonites in the alkaline complex whereas Osatenko (1979a) considered them as belonging to a separate calc-alkaline suite. These authors placed the porphyritic monzonite – leuco-monzonite contact in radically different locations on their maps. As indicated in Figure 2, these lithologies appear to comprise a single mappable unit in which rocks with porphyritic textures grade into quartz-bearing monzonites lacking potassium feldspar phenocrysts. A small body of quartz monzonite also occurs as a marginal phase of melanocratic monzonite-syenite at the northern edge of the southern cupola.

Buff to pale grey-weathering outcrops of porphyritic monzonite in the northwestern part of the northern cupola near the mela-monzonite contact are locally stained with hematite and limonite and commonly exhibit rusty patches due to disseminated sulfides (largely pyrite). A weak to moderate igneous flow lamination is locally highly variable in strike over 20-30 m of continuous outcrop but dips remain steep. A finer-grained phase with sparse potassium feldspar phenocrysts occurs near the contact with medium to coarse-grained mela-monzonite and locally carries angular to subangular xenoliths (≤1 m) and larger rafts of metasediments and mela-monzonite. Dikes of porphyritic monzonite with sharp contacts are observed cutting mela-monzonite and hornblende clinopyroxenite.

Porphyritic monzonites west of Whiterocks Mountain summit near the clinopyroxenite contact are weakly to strongly laminated and locally intercalated with thin (5-20 cm) layers of melanocratic hornblende diorite or monzodiorite and hornblende-porphyritic mela-monzonite. In the coarser layers prismatic hornblende crystals and tabular potassium feldspars reach 2.5 and 3 centimeters in length, respectively, and some trachytic-textured zones are crowded with feldspar. Xenoliths of hornblende-poor clinopyroxenite with diffuse margins have also been observed. These diverse lithologies pass westward into relatively uniform porphyritic monzonite and non-porphyritic, leucocratic quartz-bearing monzonite which commonly lack a distinct igneous fabric.

The medium to coarse-grained leucocratic quartz monzonites near the eastern margin of the intrusion are typically non-porphyritic and contain 5-10 vol. % mafics minerals and up to 19 vol. % quartz, although most appear to have less (5-10 vol. %; Mehner, 1982). Xenolith trains of hornfelsed metasedimentary rocks, some with well-developed reacton rims involving coarse-grained intergrowths of hornblende and feldspar, occur locally near the contact (Photo 3). Two samples of slightly more melanocratic monzonite (15 vol. % mafic minerals), one collected near the southern contact of the composite body, and the other from the southern cupola, contain igneous garnet.

Mineralogically, the porphyritic monzonites and quartz monzonites contain plagioclase and potassium feldspar in subequal proportions, hornblende ± biotite ± quartz and accessory magnetite, apatite and sphene. In general, the rocks are weakly altered to an assemblage of epidote + sericite + clay ± chlorite ± carbonate. Sodic plagioclase (≤4 mm) occurs as subhedral crystals with patchy and fine-scale oscillatory zoning. Euhedral to subhedral, well-twinned microcline phenocrysts exhibit patch and string perthite textures and some crystals show very fine oscillatory zoning. Potassium feldspar also forms small laths and anhedral grains in the groundmass.

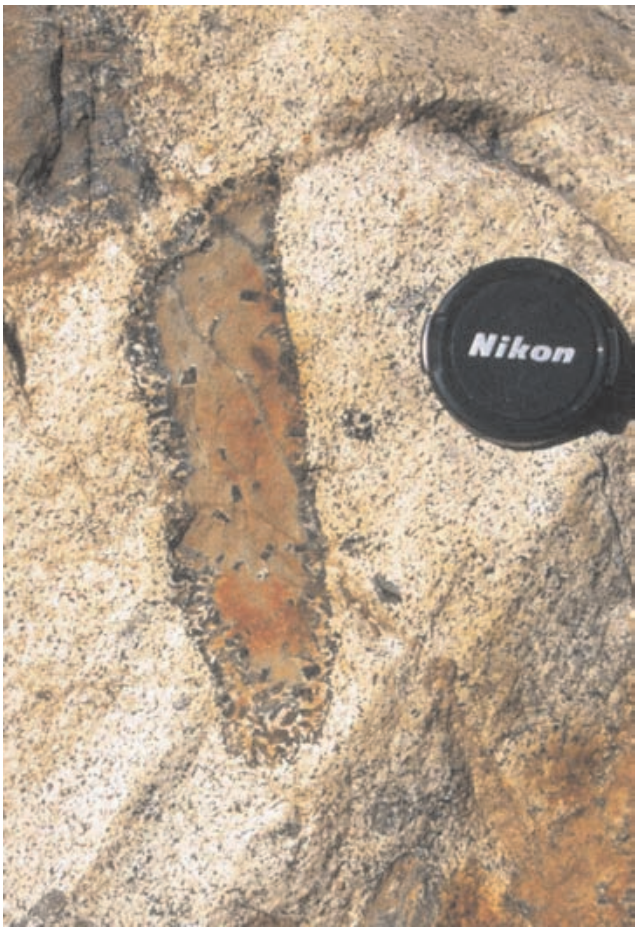

Photo 3. Metasedimentary xenolith in leucocratic quartz monzonite displaying a reaction rim of coarsely crystalline hornblende and feldspar, eastern margin of composite porphyritic monzonite – quartz monzonite unit, northern cupola, Whiterocks complex. (Pencil magnet is 13 cm in length.)

Subhedral to anhedral, pale brown to dark green pleochroic hornblende (≤4 mm) may enclose biotite and rare relict clinopyroxene, and in the more leucocratic rocks is commonly partially altered to epidote and chlorite. Quartz and colourless to pale brown biotite in the latter rocks occur in fine-grained intergrowths with feldspar. Pale pinkish brown poikilitic garnet (≤5 mm) is found in quartz-free monzonite and contains inclusions of euhedral plagioclase, microcline and apatite. Brownish subhedral sphene (≤0.7 mm), apatite and magnetite combined form less than 1 vol. % of the leucocratic rocks but are two to three times as abundant in the more melanocratic porphyritic monzonites.

Marginal Trachyte

A tan-weathering, aphanitic felsic volcanic rock, pale grey on fresh surfaces, is exposed in an area of low scattered outcrops at the southwestern margin of the northern cupola (Figure 2). The rock has a marked flow lamination and contains large (≤6 cm) vesicles lined with clay minerals and flattened parallel to the plane of flowage. This unit can be traced a short distance laterally almost to its contact with the porphyritic monzonite and clinopyroxenite where it has been hornfelsed to a pinkish grey rock with a sugary texture. Xenoliths of the hornfelsed trachyte have been observed in the porphyritic monzonite. Contacts with metasedimentary host rocks to the south appear to be hidden beneath a thin cover of glacial drift.

In thin section, a relict flow fabric is preserved amidst areas of recrystallization. Microphenocrysts of subhedral clinopyroxene (≤0.3 mm) are set in a finely crystalline groundmass of potassium feldspar, plagioclase and minor brown pleochroic hornblende. Within the contact aureole, the rock is converted to an assemblage of granular clinopyroxene, quartz and feldspar (mainly plagioclase), and has areas rich in fine-grained epidote and diffuse veins of feldspar and quartz. The rock is classified as a trachyte based on its chemical composition (presented below). It is interpreted to represent a chilled facies of the Whiterocks alkaline suite which was probably intruded as a dike, and was later subject to intrusion by the plutonic members of the suite.

Minor Intrusions

Dikes and veins observed cutting the Whiterocks complex and mineralogically similar to the main lithologies described above include hornblendite and hornblende gabbro/diorite, melanocratic monzonite, megacrystic and porphyritic monzonite-syenite, and leucocratic quartz monzonite. Other related varieties include medium to coarse-grained leuco-syenite dikes and feldspathic veins, biotitite veins (only found in clinopyroxenite), and plagioclase-clinopyroxene-hornblende porphyritic dikes. A microcline-megacrystic dike cutting clinopyroxenite contains small (<1 mm) euhedral to subhedral crystals of pinkish brown igneous garnet. A pegmatitic segregation vein in porphyritic monzonite contains muscovite with hematite lamellae along cleavage traces which indicate that it is most likely pseudomorphous after biotite, a common phase in the hostrock.

Emplacement History

The emplacement history of the Whiterocks alkaline suite has been deduced from the nature of contacts, xenoliths and crosscutting relationships. The earliest members of the suite are the clinopyroxenites, which formed by crystal accumulation, and the melanocratic monzonites. Interlayering of clinopyroxenite, hornblendite, hornblende gabbro/diorite and melanocratic monzonite on the scale of the outcrop, mutual inclusions of plastically deformed clinopyroxenite and mela-monzonite xenoliths near the contacts of map units, and the presence of mappable bodies of clinopyroxenite within mela-monzonite (Mehner, 1982; Osatenko, 1979a; not differentiated in Figure 2) indicate that there was more than one period of clinopyroxenite and mela-monzonite crystallization. At least some of the megacrystic monzonite also appears to have formed during the crystallization of mela-monzonite since composite dikes cutting clinopyroxenite in the northern cupola exhibit an early melanocratic monzonite margin and late megacrystic monzonite core (Photo 4). In the southern cupola, however, mela-monzonite intrudes megacrystic monzonite-syenite. The latter contacts are diffuse and evidently formed while the megacrystic monzonite was hot and plastic. Also, potassium feldspar megacrysts are rarely encountered in laminar zones within the mela-monzonite, and dikes of the latter are found cutting megacrystic monzonite in the northern cupola.

The porphyritic and quartz-bearing monzonites, and associated leucocratic dikes, are considered to be the youngest members of the suite. The contact of the clinopyroxenite with the large porphyritic monzonite – quartz monzonite unit in the northern cupola was originally mapped by Mehner (1982) as a foliated "gneissic"

Photo 4. Microcline-megacrystic monzonite-syenite dike containing platy xenoliths of mela-monzonite peeled off the dike margin and angular inclusions of clinopyroxenite, western margin of northern cupola, Whiterocks complex. The dike is cut by a late leuco-syenite vein (left of hammer).

hybrid zone, some 5 to 80 metres in width, incorporating coarse to medium-grained monzonite, monzodiorite, hornblende gabbro/diorite and hornblendite. According to Mehner, this zone originated by the interaction of fluids from a partially liquid porphyritic monzonite with solid pyroxenite. This zone has been re-interpreted herein to represent a transitional contact where these lithologies primarily reflect crystallization from rapidly changing parental melt compositions within the magma chamber. Locally, lithologies which comprise this zone may have experienced remobilization shortly after their deposition. As noted above, the monzonite progressively loses its porphyritic texture and becomes more leucocratic and quartz-bearing to the east, ultimately becoming a leucocratic quartz monzonite near its eastern margin with no obvious intrusive contact between the two lithologies. At the northwestern extremity of this map unit, the nature of the contact between a leucocratic sparsely porphyritic monzonite and the clinopyroxenite and mela-monzonite units to the south is quite different. Here, dikes of the porphyritic monzonite cut sharply through the more mafic units and the margin of the intrusion is locally fine-grained (aplitic). If, indeed, the porphyritic and leucocratic monzonites form a single composite intrusion, as suggested above, the clinopyroxenites and mela-monzonites on the western margin of the northern cupola must be older than equivalent rock types to the east.

MT. SANDBERG PLUTON AND OTHER INTRUSIONS

The Mt. Sandberg pluton is an elongate stock (3.5 x 1.5 km) which lies on the same north-northwesterly oriented trend as the alkaline intrusions (Photo 5). According to Rb-Sr whole-rock isochron systematics, the Mt. Sandberg pluton has an isotopic age of 147 ± 6 Ma (R. L. Armstrong *in* Mehner, 1982). Osatenko (1979a) subdivided the stock into a number of rock types including quartz porphyry, quartz monzonite, diorite and leucocratic quartz diorite (not differentiated in Figure 2).

The main lithology is a quartz- and potassium feldspar-porphyritic biotite monzogranite. Rounded quartz crystals (≤6 mm) and sparse, subhedral potassium feldspars (≤5 mm) are set in an equigranuilar, biotite-bearing (~8 vol. %) quartzofeldspathic groundmass. Locally, the cores of plagioclase crystals are partially altered to clay and sericite, and biotite is weakly chloritized. The rock is cut locally by a stockwork of quartz veins which are known to be associated with trace amounts of molybdenite mineralization (Osatenko, 1979a). Other subordinate rock types include weakly saussuritized, medium-grained, hornblende-bearing biotite quartz monzonite and dikes of sericitized biotite granodiorite and aplite.

East of Mt. Sandberg, a stock at the northern limit of the map area, informally referred to as the northern pluton, is associated with weak garnet-epidote skarn development in carbonate hostrocks with traces of pyrite, and chalcopyrite, and malachite staining. Texturally, the intrusion varies from equigranular and medium-grained biotite-quartz monzonite to a rock with similar mineralogy but carrying pink, euhedral-subhedral potassium feldspar-megacrysts (4 x 1 cm), rounded quartz crystals (≤6 mm), and flakes of biotite (≤3 mm; 10-15 vol. %). The rock appears to lack an internal primary fabric but exhibits a strong flow foliation at its margin where it entrains metasedimentary xenoliths.

A diverse suite of sills and dikes are observed cutting hostrocks of the Harper Ranch Group in the map area and include hornblende-biotite quartz monzonite, biotite-plagioclase porphyries and medium-grained, equigranular clinopyroxene-bearing diorite. The majority of these minor intrusions are probably Jurassic in age,

Photo 5. View of Mt. Sandberg across Tadpole Lake looking northwest from the Dobbin property.

the exception being the diorite which may be older (Upper Paleozoic?). In addition, Mehner (1982) mapped a suite of leucocratic quartz diorite dikes which postdate the alkaline rocks of the Whiterocks complex and, as noted above, yield uppermost Jurassic isotopic ages.

HARPER RANCH GROUP

Country rocks of the Harper Ranch Group in the map area comprise mainly interbedded metamorphosed sedimentary rocks including black to grey-green, calcareous to non-calcareous pelites (slates and phyllites), siliceous siltstones and volcaniclastic wackes, dark grey to brownish cherts and argillaceous to relatively pure carbonate units variably tranformed to marble, especially near intrusive contacts (Figure 2). The regional grade of metamorphism appears to be mid-greenschist facies but may reach upper greenschist to lowermost amphibolite grade in the vicinity of intrusive contacts. At the scale of mapping, one argillaceous limestone – marble unit in the eastern part of the map area can be traced along strike for over 5 kilometres and may be the same unit as that transected by the eastern margin of the northern pluton. In this part of the map area, thinner carbonate horizons are commonly found interbedded with the fine-grained siliciclastic rocks, and one such unit contains abundant transported crinoid ossicles (Photo 6 and Figure 2). Throughout the map area, sedimentary structures are relatively scarce. However, well-developed load-and-flame structures have been observed in a sequence of thinly bedded feldspathic wackes and siltstones near the eastern margin of the northern cupola of the Whiterocks Mountain stock where they indicate that the beds are overturned to the east (Photo 7).

STRUCTURE

The principal structural features of the Whiterocks Mountain area are shown in Figure 3 and plotted in stereonets and rose diagrams in Figure 4. The stratigraphy of the Harper Ranch Group strikes north-northwesterly, parallel to the trend of the Whiterocks Mountain – Mt. Sandberg stocks, and dips moderately to steeply westward. A strong penetrative foliation lies parallel or subparallel to bedding planes and is a transposed fabric locally containing dismembered minor fold limbs, rootless fold hinges and local mylonitic shear zones, especially within the more ductile carbonate units. Kinematic indicators, specifically C-S fabrics, indicate eastward tectonic transport (Photo 8). The foliation has been arbitrarily designated S1, although earlier fabrics may well exist. The similar attitude of bedding and foliation, the identification of beds locally overturned to the east, and eastward-directed tectonic transport in some ductile shear zones, are consistent with a northeasterly-directed compressional event involving isoclinal folding on a regional scale prior to pluton emplacement.

In contrast to the attitudes of bedding and foliation, primary igneous laminations in the Whiterocks Mountain

Photo 6. Well-preserved crinoid ossicles in thin carbonate unit, Harper Ranch Group. Fossil locality shown in Figure 2.

Photo 7. Well-developed load-and-flame structures in metasandstone-siltstone beds of the Harper Ranch Group indicating tops to the right (northeast), eastern margin of northern cupola of the Whiterocks complex. (Pencil magnet is 14 cm in length).

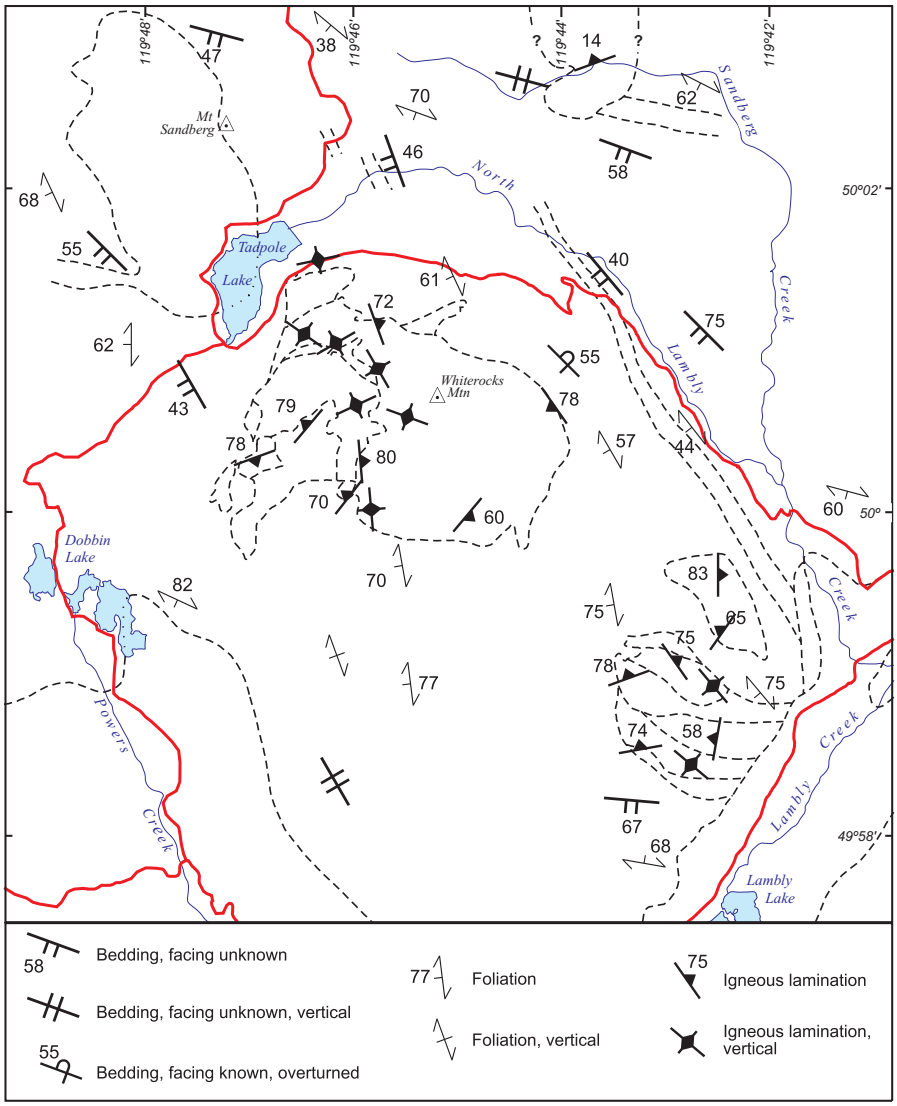

Figure 3. Generalized map of structural features in the Whiterocks Mountain area showing attitude of bedding (S0), the main foliation (S1) and igneous flow laminations within the alkaline complex.

alkaline complex show no such consistency, at least on a regional scale. The lamination, which is predominantly observed in, but not restricted to, the feldspathic rocks, has been formed by the deposition of crystals during viscous flowage and reflects the activity of convection currents in alkaline magma chambers. Locally, it may permit the reconstruction of igneous stratigraphy which would be an asset in the event that controls on sulfide mineralization are magmatic in part (discussed below).

MINERAL CHEMISTRY

A small suite of ultramafic and feldspathic rocks were selected for mineral analysis. Mineral compositions were determined by wavelength-dispersive analysis using a CAMECA SX-50 electron-microprobe at the University of British Columbia. Mineral grains were analyzed at an accelerating voltage of 15 kV and 20 nA beam current with a minimum peak-counting time of 20 s for both major and minor elements. Instrument calibration was performed on documented natural standards and standard ZAF corrections were applied to all analyses. A minimum of two spot analyses per grain were used to determine homogeneity on both a mineral and thin-section scale. Estimates of within-run accuracy and precision were determined by bracketing analyses of unknowns with analyses of international mineral standards (Table A1, Appendix).

Pyroxene

Representative analyses of pyroxenes from clinopyroxenites and hornblendites are presented in Table 1 and plotted in Figures 5 and 6 in accordance with the classification scheme of Morimoto (1989). The ferric iron content was estimated by charge balance according to stoichiometric constraints.

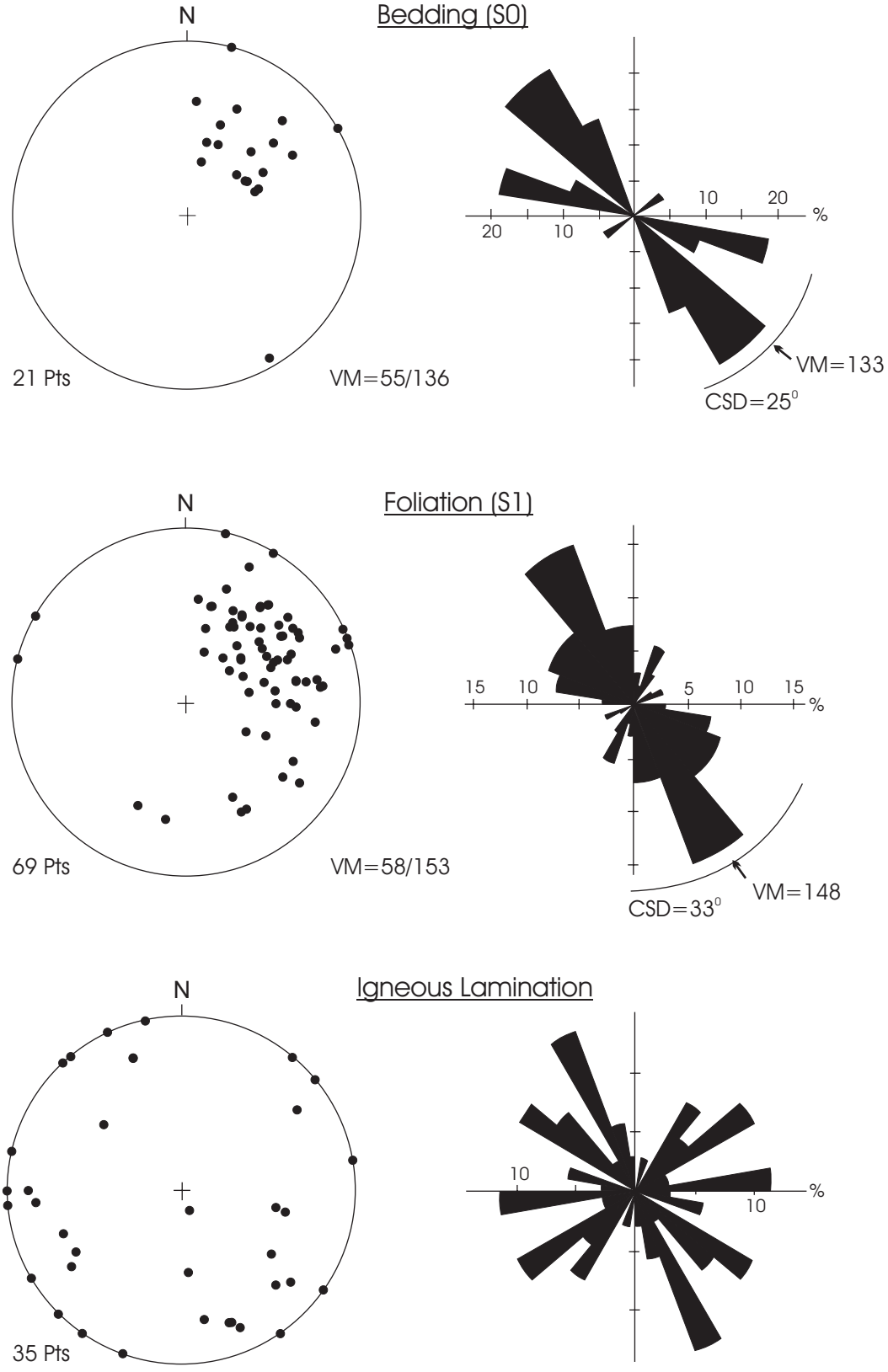

Figure 4. Equal-angle (Wulf) stereonet plots (lower hemisphere, pole to planes) and azimuth-frequency rose diagrams for structural elements in the Whiterocks Mountain area. VM, vector mean orientation; CSD, circular standard deviation. Note the concordance of bedding and foliation in the country rocks, and the lack of any preferred regional orientation for flow fabrics within the Whiterocks complex.

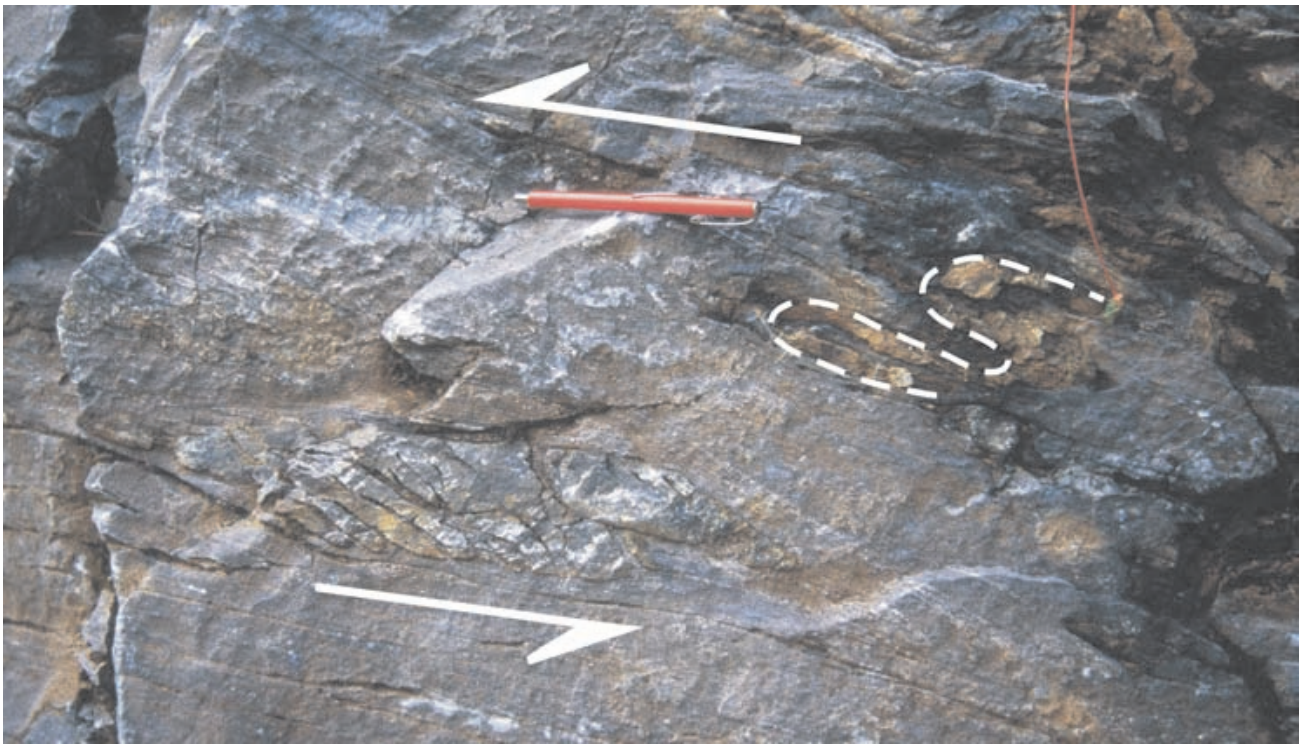

Photo 8. Rootless minor fold hinges (right of 14 cm pencil magnet) and C-S fabrics (left and lower left of magnet) in thin carbonate unit, Harper Ranch Group (unit lies structurally beneath 5 km-long carbonate layer shown in Figure 2 beyond the eastern margin of the Whiterocks complex). Both features indicate tops to the left (northeast).

All analyzed pyroxenes are high-calcium clinopyroxenes with CaO contents of 22 to 25 wt. % and Mg-numbers ($100Mg/(Mg+Fe^{2+}+Fe^{3+})$)ranging from 57 to 77. Molecular percentages of end-members (WEF) range Wo_{48-50} En_{28-40} Fs_{10-24}. As shown in Figures 5 and 6, the pyroxenes are diopsidic and plot well within the Ca-Mg-Fe quadrilateral (Quad or Q) field on the Q-J(=2Na) and WEF-Jd(jadeite)-Ae(aegirine) diagrams. The latter diagram reveals that some pyroxenes contain small amounts of the aegirine end-member but all have low Na (0.16-1.0 wt. % Na_2O). The highest Mg-numbers (~76) are found in biotite-hornblende clinopyroxenite and the lowest occur in an altered hornblende clinopyroxenite which hosts Cu-PGE sulfides and was recovered from drill core at the main Dobbin copper anomaly (DDH97-21). Significant zoning on the scale of the thin section is apparent in some samples (*e.g.* 6-4-1) though intra-grain core to rim zoning appears weak.

Amphibole

The results of the amphibole analyses in a wide range of rock types are presented in Table 2 and plotted in Figure 7. The distribution of ferrous and ferric iron has been determined using the method of Robinson *et al.* (1981) for calcic amphiboles.

According to the classification scheme of Leake *et al.* (1997), the majority of the amphiboles are either pargasite to ferropargasite ($^{VI}Al>Fe^{3+}$) in composition (Figure 7A); or magnesiohastingsite and hastingsite ($^{VI}Al<Fe^{3+}$) in composition (Figure 7B), depending on the accuracy of the Fe^{3+} recalculation. Using X-ray diffraction methods, Mehner (1982) determined that the am-

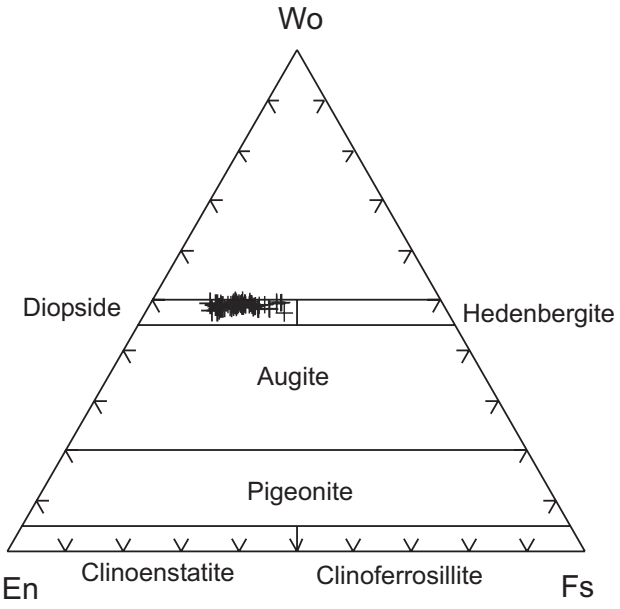

Figure 5. Wo-En-Fs (Ca-Mg-Fe) plot (mol. %) of pyroxene compositions in clinopyroxenites and hornblendites from the Whiterocks complex showing the classification scheme of Morimoto (1989). All pyroxenes fall within the diopside field.

TABLE 1
REPRESENTATIVE ELECTRON-MICROPROBE ANALYSES OF PYROXENE

Rock Type	Bi-Hb cpxite		Fs Cpx hbite		Fs Cpx hbite*		Bi-Hb cpxite		Bi cpxite	
Sample	13-5-3	13-5-3	16-2-2	16-2-2	DDH97-21-57-1		6-4-1	6-4-1	6-5-1	6-5-1
SiO_2	50.54	50.61	49.38	50.85	50.39	52.28	52.64	48.15	49.72	49.41
TiO_2	0.41	0.51	0.58	0.39	0.12	0.01	0.02	0.63	0.54	0.51
Al_2O_3	2.73	3.05	4.55	3.26	1.93	0.43	0.89	5.53	3.87	3.91
FeO	7.46	7.70	9.46	8.08	12.76	11.38	7.58	10.08	8.72	8.84
Cr_2O_3	0.02	0.00	0.03	0.01	0.00	0.06	0.03	0.00	0.00	0.00
MnO	0.25	0.17	0.34	0.38	0.44	0.57	0.29	0.37	0.32	0.38
MgO	13.84	13.55	11.40	12.76	9.64	11.07	13.60	11.38	12.57	12.55
CaO	23.34	23.68	23.18	23.42	23.57	23.66	24.50	23.31	23.77	23.95
Na_2O	0.34	0.35	0.89	0.84	0.59	0.56	0.53	0.59	0.50	0.44
Total	98.93	99.63	99.81	99.98	99.43	100.02	100.08	100.02	100.01	99.98
TSi	1.89	1.88	1.85	1.89	1.93	1.98	1.95	1.80	1.85	1.84
TAl	0.11	0.12	0.15	0.11	0.07	0.02	0.04	0.20	0.15	0.16
TFe^{3+}	0.00	0.00	0.00	0.00	0.00	0.00	0.01	0.00	0.00	0.00
M1Al	0.01	0.02	0.05	0.03	0.02	0.00	0.00	0.04	0.02	0.01
M1Ti	0.01	0.01	0.02	0.01	0.00	0.00	0.00	0.02	0.02	0.01
$M1Fe^{3+}$	0.10	0.09	0.14	0.12	0.09	0.06	0.08	0.16	0.13	0.15
$M1Fe^{2+}$	0.11	0.12	0.16	0.13	0.32	0.29	0.14	0.14	0.13	0.13
M1Cr	0.00	0.00	0.00	0.00	0.00	0.00	0.00	0.00	0.00	0.00
M1Mg	0.77	0.75	0.64	0.71	0.55	0.62	0.75	0.63	0.70	0.70
M2Mg	0.00	0.00	0.00	0.00	0.00	0.00	0.00	0.00	0.00	0.00
$M2Fe^{2+}$	0.03	0.03	0.00	0.00	0.00	0.00	0.00	0.01	0.01	0.00
M2Mn	0.01	0.01	0.01	0.01	0.01	0.02	0.01	0.01	0.01	0.01
M2Ca	0.94	0.95	0.93	0.93	0.97	0.96	0.97	0.93	0.95	0.96
M2Na	0.03	0.03	0.07	0.06	0.04	0.04	0.04	0.04	0.04	0.03
Total Cations	4.00	4.00	4.00	4.00	4.00	4.00	4.00	4.00	4.00	4.00
Mg #	76.8	75.8	68.2	73.8	57.4	63.4	76.1	66.7	72.0	71.6
Q**	1.85	1.84	1.72	1.77	1.83	1.88	1.87	1.72	1.79	1.78
J***	0.05	0.05	0.13	0.12	0.09	0.08	0.08	0.09	0.07	0.06
WO	48.01	48.65	49.63	49.02	49.84	48.88	49.42	49.28	49.20	49.26
EN	39.61	38.74	33.98	37.16	28.36	31.84	38.17	33.48	36.20	35.92
FS	12.37	12.62	16.39	13.82	21.80	19.28	12.41	17.24	14.61	14.81

Sample prefix: 00GNX. Oxides in weight percent. Number of cations calculated on the basis of 6 oxygens.
Mg# = 100Mg/(Mg+Fe2++Fe3+) Ferric iron content estimated by charge balance according to stoichiometric constraints.
* relict Cpx in sheared Bi-Act hbite. **Q = Ca+Mg+Fe^{2+} ***J = 2Na
Abbreviations: Bi, biotite; Hb, hornblende; Cpx, calcic clinopyroxene; Fs, feldspathic; Act, actinolite; cpxite, clinopyroxenite; hbite, hornblendite.

phiboles in most rocks are "ferrohastingsite". One sample, a leuco-quartz monzonite dike (16-4-1) near the summit of Whiterocks Mountain contains amphiboles zoned to edenite compositions. In general, Mg-numbers decrease from clinopyroxenites (62) through hornblendites (42) to the mela-monzonites (23-31) consistent with trends expected of rocks related by fractional crystallization. Rim and core analyses on most grains show no significant compositional zonation.

Mica

Analytical results for Fe-Mg micas in several clinopyroxenites and a biotitite pegmatitic vein are given in Table 3 and plotted in Figure 8. Mica analyses were recalculated on an anhydrous basis assuming that all iron is present as ferrous iron.

Mica compositions show a limited range of variation in Mg/(Mg+Fe) (0.75-0.50) across the boundary which formerly separated the biotite-phlogopite fields (Figure 8). The most magnesian biotites (6-5-1) exhibit a large variation in tetrahedral aluminum towards an "eastonitic" component (Figure 8). It is noteworthy that mica analyses from the biotite pegmatites have similar compositions to cumulus and intercumulus biotites occurring in host clinopyroxenites (Table 3). This indicates that the biotitite veins are igneous in origin and not hydrothermal as previously proposed by Mehner (1982). Analyses at the cores and rims of mica grainss failed to show any significant zoning.

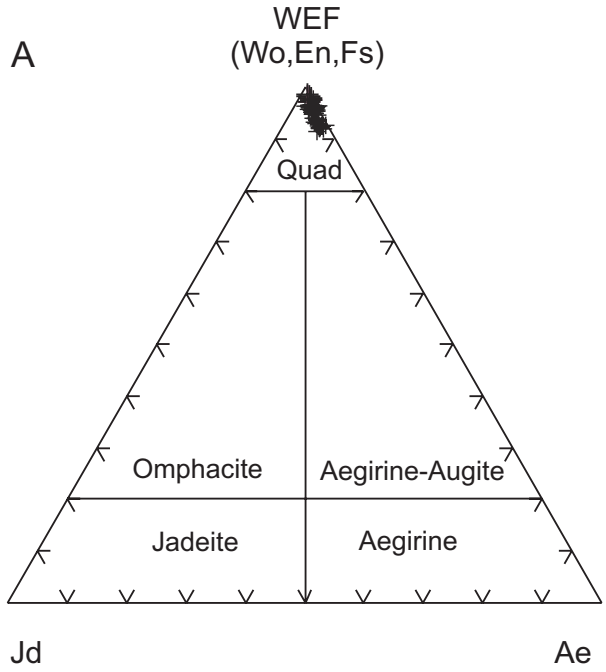

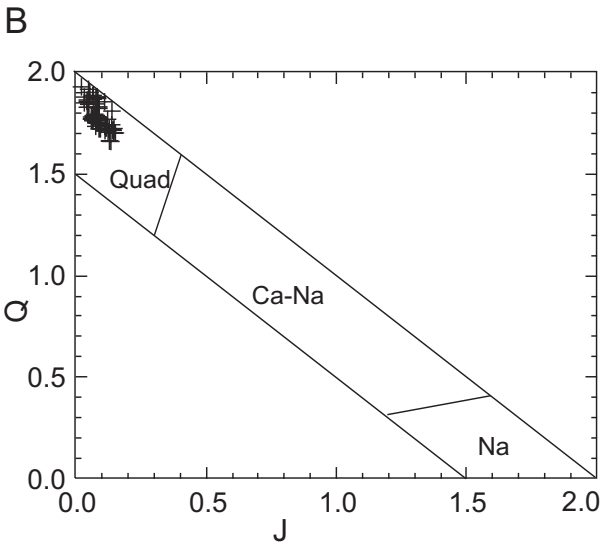

Figure 6. Classification of components other than quadrilateral constituents ("Others") in clinopyroxenes of the Whiterocks complex (after Morimoto, 1989). A, WEF-Jd-Ae and B, Q ($Ca+Mg+Fe^{2+}$) – J (2Na) plots (atoms per formula unit) showing the incorporation of small amounts of the aegirine end-member.

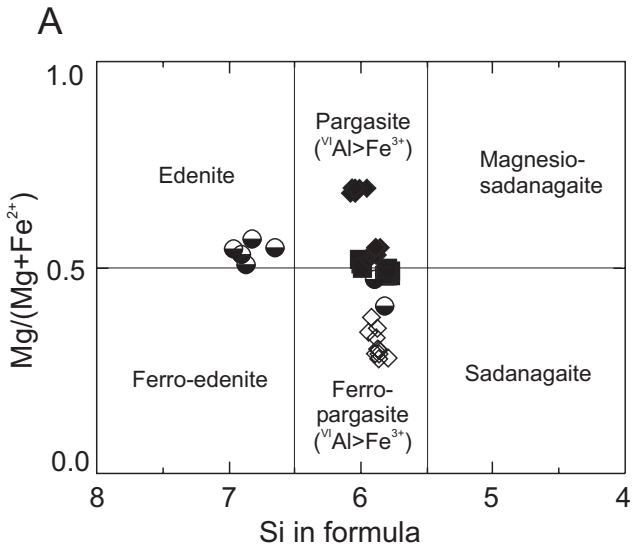

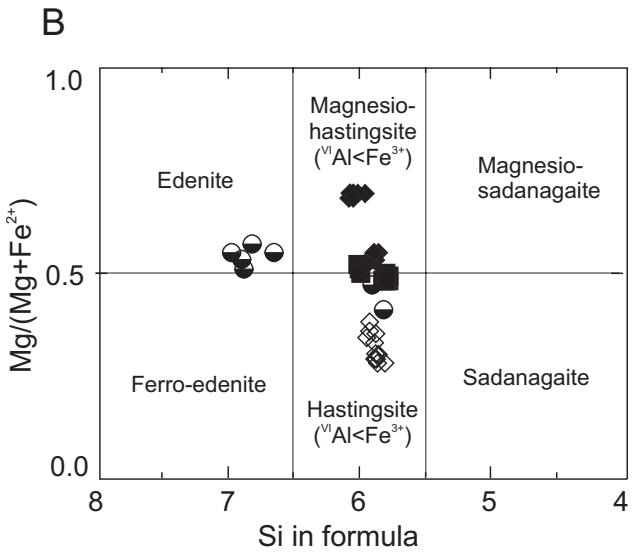

Figure 7. Classification of calcic amphiboles with CaB>1.50, (Na+K)A>0.50, and Ti<0.50 (atoms per formula unit) in selected rocks from the Whiterocks complex showing the effect of uncertainty in the amount of ferric iron (calculated after Robinson *et al.*, 1981) on the nomenclature. A, octahedral alumina is greater than ferric iron; B, octahedral alumina is less than ferric iron. Note the zoning towards edenitic compositions in the leuco-syenite dike.

Garnet

The first occurrence of garnet in the Whiterocks complex was noted by J. F. Harris in a petrographic report prepared for Verdstone/Molycor (Kikauka, 1997). The garnet was found in a leucocratic syenite vein cutting clinopyroxenite in drill core DDH97-2 (23.5 m) which was recovered from the main Dobbin copper anomaly. This sample was obtained for analysis and the results are given in Table 4. The partitioning of ferrous and ferric

TABLE 2
REPRESENTATIVE ELECTRON-MICROPROBE ANALYSES OF AMPHIBOLE

Rock Type	Bi-Hb cpxite		mKf(Gt)-Hb mmz/sy		Cpx hbite	Fspo lqmz dyke		Bi-Hb cpxite	
Sample	13-5-3	13-5-3	13-9-2	13-9-2	16-2-2	16-4-1	16-4-1	6-4-1	6-4-1
SiO_2	40.25	40.63	37.81	36.65	37.45	37.08	45.83	38.76	38.62
TiO_2	1.76	1.78	2.03	1.53	1.98	2.10	0.26	1.99	2.06
Al_2O_3	13.33	13.20	13.66	13.60	13.99	13.41	6.65	12.89	13.58
FeO	13.61	13.58	23.20	25.59	19.87	20.96	18.52	18.40	17.90
Cr_2O_3	0.01	0.06	0.00	0.00	0.02	0.05	0.00	0.00	0.03
MnO	0.13	0.15	0.70	0.89	0.51	1.53	2.48	0.40	0.32
MgO	12.38	12.42	5.76	4.38	8.17	6.55	9.89	9.38	9.79
CaO	12.28	12.17	11.22	10.96	11.40	11.29	11.24	11.48	11.66
Na_2O	1.86	1.90	1.36	1.56	1.88	1.52	1.06	2.18	2.11
K_2O	1.56	1.50	2.36	2.34	2.53	2.22	1.01	2.16	2.21
F	0.23	0.27	0.07	0.15	0.22	0.62	0.59	0.12	0.23
Cl	0.08	0.11	0.21	0.12	0.08	0.15	0.04	0.09	0.13
Total	97.47	97.71	98.38	97.77	98.09	97.43	97.57	97.85	98.60
TSi	6.01	6.05	5.88	5.80	5.77	5.82	6.96	5.94	5.86
TAl	1.99	1.96	2.12	2.20	2.23	2.18	1.05	2.06	2.14
CAl	0.35	0.36	0.38	0.34	0.31	0.30	0.14	0.27	0.28
CCr	0.00	0.01	0.00	0.00	0.00	0.01	0.00	0.00	0.00
*CFe^{3+}	0.45	0.42	0.53	0.69	0.52	0.57	0.52	0.38	0.45
CTi	0.20	0.20	0.24	0.18	0.23	0.25	0.03	0.23	0.24
CMg	2.75	2.75	1.34	1.03	1.88	1.53	2.24	2.14	2.21
CFe^{2+}	1.24	1.25	2.47	2.70	2.03	2.18	1.83	1.95	1.79
CMn	0.01	0.01	0.05	0.06	0.03	0.16	0.24	0.03	0.02
CCl	0.02	0.03	0.05	0.03	0.02	0.04	0.01	0.02	0.03
CF	0.11	0.13	0.03	0.07	0.11	0.31	0.29	0.06	0.11
BFe^{2+}	0.01	0.02	0.02	0.01	0.02	0.00	0.00	0.03	0.03
BMn	0.01	0.01	0.05	0.06	0.03	0.05	0.08	0.03	0.02
BCa	1.96	1.94	1.87	1.86	1.88	1.90	1.83	1.89	1.90
BNa	0.02	0.03	0.07	0.08	0.06	0.05	0.09	0.06	0.06
ANa	0.52	0.52	0.34	0.40	0.50	0.41	0.22	0.59	0.56
AK	0.30	0.29	0.47	0.47	0.50	0.45	0.20	0.42	0.43
Total Cations	15.82	15.80	15.81	15.88	16.00	15.86	15.42	16.01	15.99
Mg #	61.9	62.0	30.7	23.4	42.3	35.8	48.8	47.6	49.4

Sample prefix: 00GNX. Oxides in weight percent. Number of cations based on 23 oxygens. Mg# = $100Mg/(Mg+Fe^{2+}+Fe^{3+})$

*Ferric iron recalculated on an anhydrous basis by method of Robinson (1981).

Abbreviations: Bi, biotite; Hb, hornblende; Cpx, calcic clinopyroxene; Fs, feldspar; Gt, garnet; mKf, megacrystic (>2.5 cm) potassium feldspar; m, melanocratic; l, leucocratic; cpxite, clinopyroxenite; mz, monzonite; qmz, quartz monzonite; sy, syenite; po, porphyritic.

iron in garnet was handled by the empirical formulation of Knowles (1987).

The analyzed garnets are pinkish brown, subhedral to euhedral crystals with broad birefringent rims which possess fine-scale oscillatory zoning. Compositions are andradite and andradite-grossular solid solutions, with 65-81 mol. % andradite, 15-32 mol. % grossular and <3 mol. % each of almandine, spessartine, and pyrope components (Table 4). Of note are the TiO_2 contents of these garnets which range from 0.43-1.8 wt. % and thus become melanitic (TiO_2 >1 wt. %). The high-Ti compositions are predominantly core analyses and appear to correlate with elevated abundances of MnO (>1 wt. %). Except for their birefringent, oscillatory-zoned mantles, which may be related to late carbonate-epidote alteration in this sample, these crystals appear optically similar to igneous garnets encountered elsewhere in the suite.

Feldspar

Several monzonitic samples from the suite were analyzed for plagioclase and potassium feldspar. The results are given in Table 5 and plotted in Figure 9. Most of the feldspars analyzed have cumulus and intercumulus textures, and large cumulus grains generally show oscillatory zoning. Such zoning in these crystals, however, appears to be weak since core to rim microprobe traverses did not detect appreciable compositional variation.

The alkali feldspar compositions are all microcline, and the majority of plagioclase compositions range from sodic oligoclase to sodic andesine, with minor albite.

TABLE 3
REPRESENTATIVE ELECTRON-MICROPROBE ANALYSES OF MICA

Rock Type	Biotitite vein in Bi-Hb cpxite		Bi-Hb cpxite		Biotitite vein in Bi-Hb cpxite		Bi cpxite	
Sample	13-5-3	13-5-3	6-4-1	6-4-1	6-4-2	6-4-2	6-5-1	6-5-1
SiO_2	36.06	36.21	35.91	35.94	35.74	36.16	36.86	34.89
TiO_2	2.11	1.81	1.54	0.00	2.07	1.89	2.27	3.95
Al_2O_3	15.55	14.87	14.94	15.70	14.71	14.93	16.15	17.09
FeO	10.92	14.18	19.30	22.09	16.28	15.23	10.94	13.18
Cr_2O_3	0.00	0.04	0.01	0.00	0.10	0.10	0.00	0.02
MnO	0.19	0.11	0.32	0.00	0.25	0.20	0.22	0.38
MgO	18.44	16.82	12.46	12.27	14.25	14.94	17.70	16.81
CaO	0.14	0.06	0.03	0.02	0.03	0.00	0.00	0.04
Na_2O	0.25	0.26	0.16	0.12	0.16	0.20	0.20	0.21
K_2O	9.38	9.55	9.77	10.05	9.90	9.86	9.70	9.30
F	0.50	0.43	0.12	0.00	0.38	0.23	0.25	0.34
Cl	0.05	0.07	0.03	0.00	0.01	0.02	0.02	0.04
Total	93.59	94.41	94.58	96.20	93.88	93.77	94.31	96.24
Si	5.44	5.50	5.57	5.53	5.53	5.55	5.49	5.17
Al^{IV}	2.57	2.50	2.44	2.47	2.47	2.45	2.51	2.83
Al^{VI}	0.20	0.16	0.29	0.38	0.21	0.25	0.32	0.15
Ti	0.24	0.21	0.18	0.00	0.24	0.22	0.25	0.44
$*Fe^{2+}$	1.38	1.80	2.50	2.84	2.11	1.95	1.36	1.63
Cr	0.00	0.01	0.00	0.00	0.01	0.01	0.00	0.00
Mn	0.02	0.01	0.04	0.00	0.03	0.03	0.03	0.05
Mg	4.14	3.81	2.88	2.81	3.28	3.42	3.93	3.71
Ba	0.00	0.00	0.00	0.00	0.00	0.00	0.00	0.00
Ca	0.02	0.01	0.01	0.00	0.01	0.00	0.00	0.01
Na	0.07	0.08	0.05	0.04	0.05	0.06	0.06	0.06
K	1.80	1.85	1.93	1.97	1.95	1.93	1.84	1.76
Cations	15.88	15.92	15.88	16.05	15.89	15.87	15.79	15.81
CF	0.47	0.41	0.12	0.00	0.38	0.23	0.23	0.32
CCl	0.03	0.04	0.02	0.00	0.01	0.01	0.01	0.02
Fe^{2+}/Mg	0.33	0.47	0.87	1.01	0.64	0.57	0.35	0.44
Mg #	0.75	0.68	0.54	0.50	0.61	0.64	0.74	0.69
X	1.90	1.94	1.99	2.01	2.01	1.99	1.90	1.82
Y	5.72	5.76	5.67	6.03	5.59	5.62	5.61	5.49
Z	8.00	8.00	8.00	8.00	8.00	8.00	8.00	8.00

Sample prefix: 00GNX. Oxides in weight percent. Number of cations based on 22 oxygens.
X = K+Na+Ca, Y = $Mg+Fe^{2+}+Al^{VI}$, Z = $Si+Al^{IV}$ Mg # = $Mg/(Mg+Fe^{2+})$
Abbreviations: Hb, hornblende; Bi, biotite; cpxite, clinopyroxenite.

There is a range of coexisting feldspar compositions for each rock type. In the leuco-quartz monzonite (10-4-1), potassium feldspar compositions of Or_{87}-Or_{96} coexist with plagioclase of Ab_{78}-Ab_{96}. A porphyritic garnet-bearing mela-monzonite (13-9-2) has potassium feldspar compositions of Or_{82}-Or_{95} coexisting with plagioclase of Ab_{61}-Ab_{81}; and a leuco-monzonite dike (16-4-1) contains potassium feldspar compositions of Or_{91}-Or_{97} and coexisting plagioclase of Ab_{70}-Ab_{96}.

Summary of Electron-Microprobe Results

The electron-microprobe analyses permit for a quantitative characterization of the mineralogy of the Whiterocks complex. All pyroxenes are high-Ca clinopyroxenes of diopsidic composition as opposed to aegirine augite (Mehner, 1982). Amphibole compositions are pargasite to ferro-pargasite, or magnesio-hastingsite to hastingsite depending on the accuracy of the ferric iron recalculation. Ferromagnesian micas straddle the boundary which formerly defined phlogopite-biotite compositions; the compositions of pegmatitic mica in biotitite veins in clinopyroxenite, together with inclusions of euhedral apatite and relict clinopyroxene, indicate that the biotitites are magmatic as opposed to hydrothermal in origin and unrelated to the mineralization. Megacrysts of alkali feldspar in monzonitic rocks are low-temperature microclines. The textural relationships and melanitic composition of garnet in monzonitic rocks of the complex confirm an igneous origin for the garnet.

TABLE 4
REPRESENTATIVE ELECTRON-MICROPROBE ANALYSES OF GARNET

Rock Type	Syenite vein in Hb cpxite					
Sample	DDH97-2 (23.5 m)					
SiO_2	35.25	35.49	35.54	35.91	35.53	35.50
TiO_2	1.04	0.82	0.93	0.43	0.67	0.64
Al_2O_3	4.92	5.67	7.78	8.21	7.72	7.90
FeO	22.13	22.25	19.75	20.42	20.50	20.36
Cr_2O_3	0.06	0.05	0.02	0.00	0.00	0.00
MnO	1.23	1.30	0.26	0.32	0.23	0.24
MgO	0.07	0.09	0.03	0.04	0.02	0.04
CaO	32.84	32.63	34.14	33.94	33.93	33.54
Na_2O	0.00	0.02	0.00	0.03	0.01	0.00
Total	97.54	98.33	98.46	99.29	98.61	98.23
*FeO(calc)	1.11	1.11	0.99	1.02	1.03	1.02
*Fe_2O_3(calc)	23.36	23.49	20.85	21.55	21.64	21.49
Total(calc)	99.82	100.62	100.52	101.44	100.77	100.38
TSi	2.92	2.91	2.88	2.88	2.88	2.88
TAl	0.08	0.09	0.12	0.12	0.13	0.12
Al^{VI}	0.40	0.46	0.62	0.66	0.61	0.64
Fe^{3+}	1.45	1.45	1.27	1.30	1.32	1.31
Ti	0.07	0.05	0.06	0.03	0.04	0.04
Cr	0.00	0.00	0.00	0.00	0.00	0.00
Fe^{2+}	0.08	0.08	0.07	0.07	0.07	0.07
Mg	0.01	0.01	0.00	0.00	0.00	0.01
Mn	0.09	0.09	0.02	0.02	0.02	0.02
Ca	2.91	2.86	2.96	2.92	2.94	2.92
Na	0.00	0.00	0.00	0.01	0.00	0.00
Total Cations	8.00	8.00	8.00	8.00	8.00	8.00
Alm	2.48	2.50	2.19	2.27	2.29	2.30
And	75.79	74.00	65.15	65.54	66.88	65.92
Gross	18.43	19.88	31.87	31.18	30.18	31.07
Pyrope	0.28	0.36	0.12	0.14	0.09	0.16
Spess	2.80	2.97	0.58	0.71	0.51	0.56
Uvaro	0.20	0.18	0.08	0.00	0.00	0.00
XCa	0.64	0.64	0.69	0.68	0.68	0.68
XFe	0.34	0.34	0.31	0.32	0.32	0.32
XMg	0.00	0.00	0.00	0.00	0.00	0.00

Sample prefix: 00GNX. Oxides in weight percent. Number of cations based on 12 oxygens.
*Ferrous and ferric iron recalculated after Knowles (1987).
XCa=Ca/(Ca+Mg+Fe^{2+}+Fe^{3+}+Mn); XFe=(Fe^{2+}+Fe^{3+})/(Ca+Mg+Fe^{2+}+Fe^{3+}+Mn);
XMg=Mg/(Ca+Mg+Fe^{2+}+Fe^{3+}+Mn)

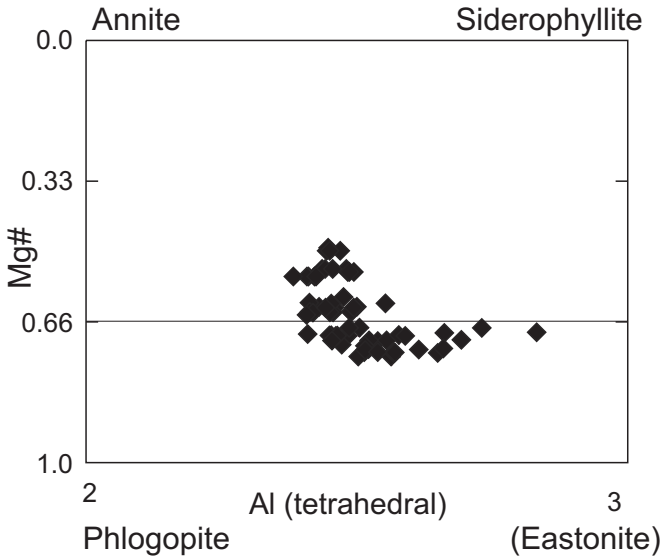

Figure 8. Mg# [Mg/(Mg+Fe)] versus tetrahedral Al plot (atoms per formula unit) for Fe-Mg mica compositions in clinopyroxenites of the Whiterocks complex. The horizontal line represents the former division (obsolete) between the compositional fields of phlogopite and biotite.

TABLE 5
REPRESENTATIVE ELECTRON-MICROPROBE ANALYSES OF FELDSPAR

Rock Type	Kfpo (Hb) lqmz			mKf(Gt)-Hb mmz/sy			Fspo lmz	
Sample	10-4-1	10-4-1	13-9-2	13-9-2	13-9-2	13-9-2	16-4-1	16-4-1
Mineral	Kf	Pl	Pl	Pl	Kf	Kf	Kf	Pl
SiO_2	65.02	63.65	59.02	64.43	64.61	64.36	65.33	64.32
Al_2O_3	18.39	23.11	26.30	22.88	18.59	19.25	18.38	22.63
FeO	0.04	0.14	0.01	0.05	0.01	0.12	0.10	0.39
MgO	0.00	0.00	0.00	0.00	0.00	0.00	0.00	0.00
CaO	0.00	4.07	7.96	3.86	0.02	0.49	0.01	3.52
Na_2O	0.62	9.17	6.84	9.43	0.60	1.71	1.00	9.32
K_2O	16.29	0.13	0.08	0.13	16.22	13.84	15.62	0.23
Total	100.37	100.27	100.22	100.79	100.05	99.78	100.43	100.42
Si	11.99	11.22	10.51	11.28	11.95	11.85	12.00	11.31
Al	3.99	4.80	5.51	4.72	4.05	4.17	3.98	4.69
Fe	0.01	0.02	0.00	0.01	0.00	0.02	0.02	0.06
Mg	0.00	0.00	0.00	0.00	0.00	0.00	0.00	0.00
Ca	0.00	0.77	1.52	0.72	0.00	0.10	0.00	0.66
Na	0.22	3.13	2.36	3.20	0.22	0.61	0.36	3.18
K	3.83	0.03	0.02	0.03	3.83	3.25	3.66	0.05
Total Cations	20.04	19.96	19.92	19.97	20.04	19.99	20.01	19.95
Ab	5.50	79.70	60.60	81.00	5.30	15.40	8.80	81.60
An	0.00	19.60	38.90	18.30	0.10	2.50	0.00	17.10
Or	94.50	0.80	0.50	0.80	94.60	82.10	91.10	1.30

Sample prefix: 00GNX. Oxides in weight percent. Number of cations based on 32 oxygens.
Abbreviations: Hb, hornblende; Gt, garnet; Fs, feldspar; Pl, plagioclase; mKf, megacrystic (>2.5 cm) potassium feldspar; Kfpo, porphyritic (<2.5 cm) potassium feldspar; m, melanocratic; l, leucocratic mz, monzonite; qmz, quartz monzonite; sy, syenite; po, porphyritic.

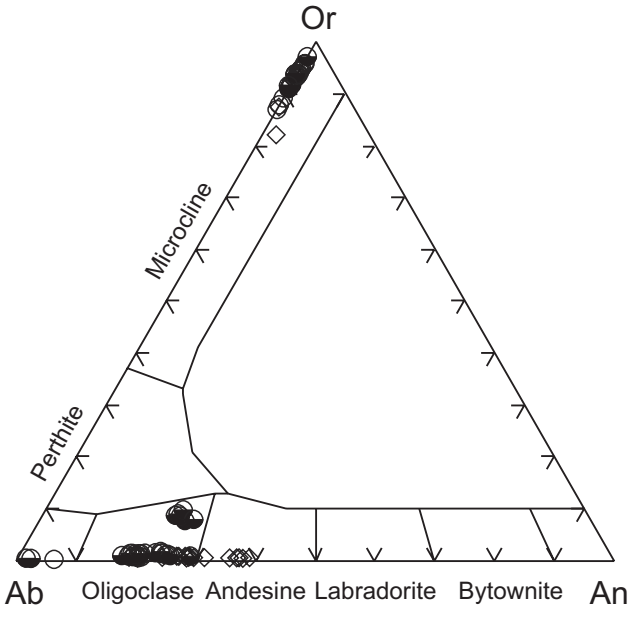

Figure 9. Or-Ab-An plot (mol. %) of potassium feldspar and plagioclase compositions in selected feldspathic lithologies of the Whiterocks complex. Open circles are leuco-quartz monzonite 10-4-1 (Table 5); other symbols as in Figure 7.

WHOLE-ROCK GEOCHEMISTRY

A suite of 58 rock samples representing a broad range of rock types from the Whiterocks Mountain alkaline complex, the Mt Sandberg pluton, and associated minor intrusions were analyzed for major elements by X-ray fluorescence at the Cominco Research Laboratory, Vancouver. Rocks were crushed in a hardened-steel jaw crusher and selected chips were reduced to <150 mesh powder in a tungsten carbide swingmill. A quartz sand wash was done between samples to prevent cross-contamination. Rock powders were dissolved in a lithium tetraborate fusion mixture using standard calibration and data reduction procedures. Accuracy and precision were monitored by international standards included in the run. The analytical results are listed according to map unit in Table 6 which also provides a summary of pertinent petrographic features for the analyzed rocks. The classification of rock types given in Table 6 were derived from visual estimates of mineral abundances using the modal classification scheme of Le Maitre *et al.* (1989). The CIPW-normative compositions of the analyzed rocks are plotted in Figure 10 and sample locations are shown in Figure 11.

Feldspathic Rocks

The QAP ternary diagram in Figure 10 provides a more quantitative and systematic basis for classifying and comparing the various petrographic groupings. Since

TABLE 6
WHOLE-ROCK MAJOR ELEMENT ANALYSES OF THE WHITEROCKS MOUNTAIN ALKALINE COMPLEX AND OTHER IGNEOUS ROCKS

ID	Sample	Rock Type	NAD 1983 Easting	NAD 1983 Northing	SiO_2	TiO_2	Al_2O_3	Fe_2O_3t	MnO	MgO	CaO	Na_2O	K_2O	P_2O_5	LOI	Total
Whiterocks Mountain Alkaline Complex																
Clinopyroxenite																
34	00GNX-1-1-1	Bi-Hb cpxite (Ap≤0.4)	301595	5542706	42.00	1.04	7.50	16.51	0.28	10.73	17.62	0.73	1.17	0.94	0.93	99.45
16	00GNX-16-1-1	fBi-Hb cpxite (Ap≤0.3)	301897	5543695	40.29	1.25	9.81	17.90	0.30	9.14	16.82	0.77	1.44	0.92	0.60	99.24
56	00GNX-13-8-1	Hb-Bi cpxite (Ap≤0.4)	305006	5539428	40.04	1.41	6.00	19.71	0.27	11.10	17.34	0.44	1.41	1.24	0.40	99.36
22	00GNX-16-2-8	Bi-Hb cpxite (Ap≤0.6)	301945	5543412	39.40	1.17	6.07	20.87	0.33	9.98	17.47	0.47	1.50	1.61	0.33	99.20
58	00GNX-13-5-1	Bi-Hb cpxite (Ap≤0.5)	305525	5539076	39.17	1.38	6.96	20.80	0.33	9.74	16.31	0.82	1.64	1.51	0.61	99.27
33	00GNX-21-1050	fHb cpxite (Ap≤1.2)	300762	5542803	38.31	1.42	6.96	21.80	0.31	8.21	19.26	0.47	0.55	1.69	0.49	99.47
29	00GNX-1-5-1	fHb cpxite (Ap≤1.3)	301968	5542895	37.58	1.75	9.71	22.76	0.55	7.26	15.25	1.49	1.29	1.39	0.82	99.85
21	00GNX-6-4-1	Bi-Hb cpxite (Ap≤0.7)	301252	5543441	37.33	1.30	6.32	23.86	0.31	9.60	15.72	0.66	1.67	1.70	0.60	99.07
18	00GNX-6-5-1	Bi cpxite (Ap≤0.7)	301284	5543472	37.00	1.47	5.26	24.71	0.28	10.55	17.51	0.41	0.93	1.20	0.15	99.47
Hornblendite																
23	00GNX-16-2-5	Cpx hbite (Ap≤0.8)	301945	5543412	39.79	1.13	7.17	20.40	0.41	8.52	18.20	0.93	0.85	1.53	0.31	99.24
24	00GNX-16-2-1	fCpx hbite (Ap≤0.8)	301945	5543412	36.74	1.57	9.34	25.21	0.47	7.13	14.78	1.11	1.14	0.87	0.82	99.18
Melanocratic Monzonite-Syenite																
44	00GNX-12-3-1	Hb mz	306325	5540518	56.86	0.68	17.95	6.44	0.17	1.91	6.55	4.07	3.58	0.27	0.75	99.23
52	00GNX-13-9-2	mKf (Gt)-Hb mmz/sy	304861	5539524	56.77	0.34	20.03	4.61	0.12	0.87	5.82	4.80	4.40	0.15	0.85	98.76
14	00GNX-7-15-2	(Cpx)-Hb mz	301440	5544241	56.15	0.61	14.84	7.82	0.14	3.16	6.53	3.01	5.80	0.38	0.54	98.98
53	00GNX-13-9-3	(Cpx)-(Gt)-Hb mz	304861	5539524	55.31	0.40	20.62	5.34	0.15	0.92	7.53	5.26	2.75	0.18	1.01	99.47
27	00GNX-6-1-1	Gt-Hb-Cpx mmz	301149	5543349	53.56	0.60	16.90	8.15	0.18	2.45	6.98	3.65	5.71	0.43	0.68	99.29
57	00GNX-13-3-1	(Cpx)-Bi-Gt-Hb mmz	305515	5539246	53.13	0.56	17.04	8.09	0.18	2.51	6.55	4.05	5.67	0.44	1.25	99.47
13	00GNX-7-5-1	Hb-Cpx mmz	301865	5544269	52.00	0.75	16.25	9.96	0.18	3.23	8.25	3.42	4.28	0.50	0.41	99.23
54	00GNX-13-9-1	mKf (Gt)-Hb mmz/sy	304863	5539522	49.90	0.88	16.85	11.01	0.34	2.31	8.61	3.49	3.99	0.37	1.35	99.10
45	00GNX-11-17-1	Cpx-Hb mmz	305416	5540484	48.25	0.76	15.72	11.81	0.27	3.54	10.43	2.98	3.27	0.70	1.30	99.03
Kf-Megacrystic Monzonite/Syenite																
47	00GNX-11-15-2	mKf Bi mz/sy	304813	5540468	60.62	0.22	19.66	2.64	0.10	0.44	2.08	5.26	7.37	0.07	1.15	99.61
48	00GNX-11-15-6	mKf Bi mz/sy	304813	5540468	58.36	0.27	19.23	3.97	0.10	0.82	3.25	4.61	7.03	0.15	1.63	99.42
49	00GNX-11-15-1	mKf Bi mz/sy	304813	5540468	57.45	0.42	18.97	5.40	0.19	0.86	3.14	4.56	7.13	0.18	1.23	99.53
32	00GNX-17-3-1	mKf Cpx-Hb mmz	300661	5542831	51.09	0.93	17.19	10.56	0.20	2.55	9.64	3.34	3.29	0.56	0.44	99.79
30	00GNX-17-2-1	mKf Cpx-Hb mmz	300661	5542870	49.45	0.82	17.87	10.43	0.20	2.93	10.25	2.71	3.44	0.50	0.75	99.35
Kf-Porphyritic Monzonite/Quartz Monzonite																
41	00GNX-10-3-1	Kfpo Hb lqmz	303472	5542038	68.70	0.14	16.63	1.49	0.05	0.17	1.74	4.92	4.75	0.01	0.62	99.22
28	00GNX-10-4-1	Kfpo (Hb) lqmz	303774	5543018	67.44	0.15	17.45	1.50	0.05	0.18	2.23	5.00	5.07	0.02	0.37	99.46
25	00GNX-10-5-2	Hb lmz/qmz	304024	5543374	64.51	0.25	17.77	2.65	0.08	0.42	3.06	4.96	5.01	0.06	0.69	99.46
12	00GNX-7-4-1	Kfpo Hb lmz	301917	5544337	62.00	0.31	18.88	3.00	0.10	0.46	3.79	5.23	4.71	0.07	0.92	99.47
11	00GNX-7-12-1	Kfpo Hb lmz	301487	5544347	61.22	0.33	19.17	3.26	0.12	0.44	4.28	5.32	4.80	0.07	0.61	99.62
39	00GNX-2-1-1	Kfpo Hb mz	302005	5542321	58.29	0.37	19.52	4.80	0.15	1.10	4.76	5.23	4.73	0.18	0.56	99.69
40	00GNX-10-2-1	(Bi)-Gt-Hb mz	303093	5542176	55.43	0.43	19.23	5.88	0.18	1.52	6.44	4.76	4.32	0.28	0.60	99.07
35	00GNX-2-5-1	Kfpo Hb mz	301801	5542632	55.05	0.56	18.79	6.60	0.20	1.40	6.53	3.55	5.63	0.25	0.63	99.19
51	00GNX-13-1-1	Kfpo Gt-Bi mz	305753	5539563	54.83	0.51	18.30	6.57	0.20	1.24	6.46	4.17	5.96	0.23	0.98	99.45
Quartz-monzonite																
42	00GNX-11-19-1	Bi lqmz	305349	5540779	64.12	0.28	18.39	2.90	0.07	0.57	1.98	5.00	4.78	0.07	1.23	99.39
43	00GNX-11-18-1	Hb lqmz	305365	5540610	63.45	0.25	17.80	3.00	0.10	0.50	3.07	4.90	5.40	0.05	0.88	99.40
Marginal Trachyte																
36	00GNX-2-4-1	Cpx hornfels in trachyte	301754	5542623	69.48	0.41	11.43	3.60	0.03	1.64	8.17	2.85	1.34	0.09	0.18	99.22
37	00GNX-2-2-1	trachyte	301628	5542502	63.13	0.75	13.85	4.25	0.02	2.18	4.21	3.07	6.57	0.14	1.00	99.17

TABLE 6 CONTINUED
WHOLE-ROCK MAJOR ELEMENT ANALYSES OF THE WHITEROCKS MOUNTAIN ALKALINE COMPLEX AND OTHER IGNEOUS ROCKS

ID	Sample	Rock Type	NAD 1983 Easting	NAD 1983 Northing	SiO_2	TiO_2	Al_2O_3	Fe_2O_3t	MnO	MgO	CaO	Na_2O	K_2O	P_2O_5	LOI	Total
Minor Intrusions in the Whiterocks Complex																
17	00GNX-16-4-1	Fspo lqmz dyke	302588	5543533	68.33	0.11	16.87	1.40	0.05	0.18	2.27	5.07	4.67	0.01	0.49	99.45
46	00GNX-11-17-2	lsy dyke	305416	5540484	63.38	0.10	18.70	1.25	0.03	0.38	1.37	4.59	8.77	0.05	0.77	99.39
55	00GNX-13-2-1	Ms sy pegmatitic vein	305937	5539450	62.31	0.05	21.56	0.63	0.01	0.05	0.66	5.21	8.36	0.01	0.86	99.71
6	00GNX-9-10-1	Kfpo Hb mz dyke	301121	5545016	59.61	0.41	18.50	4.61	0.11	0.83	4.46	4.88	5.01	0.14	0.76	99.32
15	00GNX-6-9-1	mKf (Cpx)-Gt-Hb mz dyke	301369	5543867	54.02	0.56	18.29	7.25	0.23	1.59	6.61	3.50	6.09	0.25	0.69	99.08
31	00GNX-17-2-3	(Cpx)-Bi-Hb mmz dyke	300661	5542870	50.22	0.86	13.92	12.11	0.23	5.55	9.63	2.92	2.72	0.61	0.87	99.64
20	00GNX-16-6-1	Hb mdi/mmzdi dyke?	301838	5543463	48.95	0.82	14.97	11.82	0.25	4.34	10.55	2.73	3.60	0.66	0.46	99.15
50	00GNX-11-15-3	Plpo Cpx-Hb mmz dyke	304813	5540468	47.47	0.91	15.90	12.47	0.30	3.64	10.47	3.39	2.82	0.66	1.00	99.03
19	00GNX-16-5-1	Cpx-Hb-Pl po dyke	301885	5543465	45.11	0.56	19.50	11.05	0.21	2.97	12.31	2.64	2.07	0.47	2.14	99.03
Mt Sandberg Pluton																
8	00GNX-3-17-5	aplite dyke	298672	5544978	76.61	0.05	13.48	0.55	0.01	0.05	0.83	5.67	1.16	0.01	1.03	99.45
4	00GNX-8-8-1	Qzpo Bi mzg	300410	5545630	71.47	0.25	14.71	2.00	0.03	0.62	2.05	4.07	3.59	0.09	0.67	99.55
5	00GNX-8-10-1	Kfpo Bi mzg	299416	5545520	69.66	0.25	15.35	2.47	0.07	0.85	2.41	4.46	2.93	0.11	1.05	99.61
7	00GNX-3-17-6	Bi gd dyke*	298671	5544978	69.19	0.31	16.21	2.18	0.03	0.79	2.11	4.92	2.22	0.10	1.40	99.46
2	00GNX-4-8-1	(Hb)-Bi mzg	299117	5546771	67.47	0.34	16.04	3.17	0.07	1.00	2.90	4.75	2.55	0.18	1.04	99.51
Minor Intrusions																
38	00GNX-1-8-1	Hb-Bi qmz dyke/sill	301181	5542444	69.65	0.28	15.56	2.31	0.03	0.70	2.74	4.57	2.54	0.09	1.07	99.54
10	00GNX-11-1-2	Bi-Pl po dyke	304367	5544850	68.66	0.31	15.84	2.50	0.05	1.05	3.02	4.73	2.38	0.10	0.94	99.58
3	00GNX-9-5-1	Bi-Pl po sill	302346	5546104	63.88	0.58	15.77	4.84	0.10	1.67	4.40	3.00	3.25	0.23	1.36	99.08
9	00GNX-9-12-1	Cpx di sill**	303749	5544891	50.36	0.86	15.85	9.35	0.14	9.18	6.40	4.07	0.85	0.20	1.94	99.20
Northern Pluton																
1	00GNX-5-9-1	Bi mzg	304496	5547973	70.01	0.33	15.18	2.66	0.05	0.79	2.65	3.54	3.64	0.11	0.81	99.77
Xenolith																
26	00GNX-10-5-1	recrystallized xenolith	304024	5543373	54.08	0.97	14.69	9.38	0.21	4.26	5.07	2.81	5.92	0.25	1.08	98.72
	Standard MRG-1	(in house)			39.04	3.77	8.39	17.95	0.15	13.52	14.73	0.75	0.17	0.07	1.39	99.93
	Rec. value***				39.32	3.69	8.5	17.82	0.17	13.49	14.77	0.71	0.18	0.06		
	Standard SY-3	(in house)			59.56	0.14	11.64	6.48	0.31	2.67	8.26	4.05	4.15	0.54	1.23	99.03
	Standard SY-3	(in house)			59.68	0.15	11.68	6.48	0.31	2.68	8.27	4.07	4.15	0.52	1.17	99.16
	Standard SY-3	(hidden)			59.56	0.15	11.67	6.46	0.31	2.65	8.26	4.07	4.15	0.52	1.25	99.05
	Standard SY-3	Average			59.60	0.15	11.67	6.47	0.31	2.67	8.26	4.06	4.15	0.53	1.22	99.09
	Rec. value***				59.68	0.15	11.80	6.42	0.32	2.67	8.26	4.15	4.20	0.54		

Fe_2O_3t = total Fe as Fe_2O_3 * sericitized ** sericite-actinolite alteration *** anhydrous basis (Abbey, 1979) ID, samples located on Figure 11

Abbreviations: Hb, hornblende; Bi, biotite; Cpx, calcic clinopyroxene; Gt, garnet; Qz, quartz; Ap, apatite (apatite grain size given in millimetres); mKf, megacrystic (>2.5 cm) potassium feldspar; Kfpo, porphyritic (<2.5 cm) potassium feldspar; Pl, plagioclase; f, feldspathic; m, melanocratic (mela-); l, leucocratic (leuco-); cpxite, clinopyroxenite; hbite, hornblendite; di, diorite; mz, monzonite; mzdi, monzodiorite; qmz, quartz monzonite; gd, granodiorite; sy, syenite; mzg, monzogranite; po, porphyry or porphyritic. Brackets indicate mineral present in low (trace-1 vol. %) modal proportions.

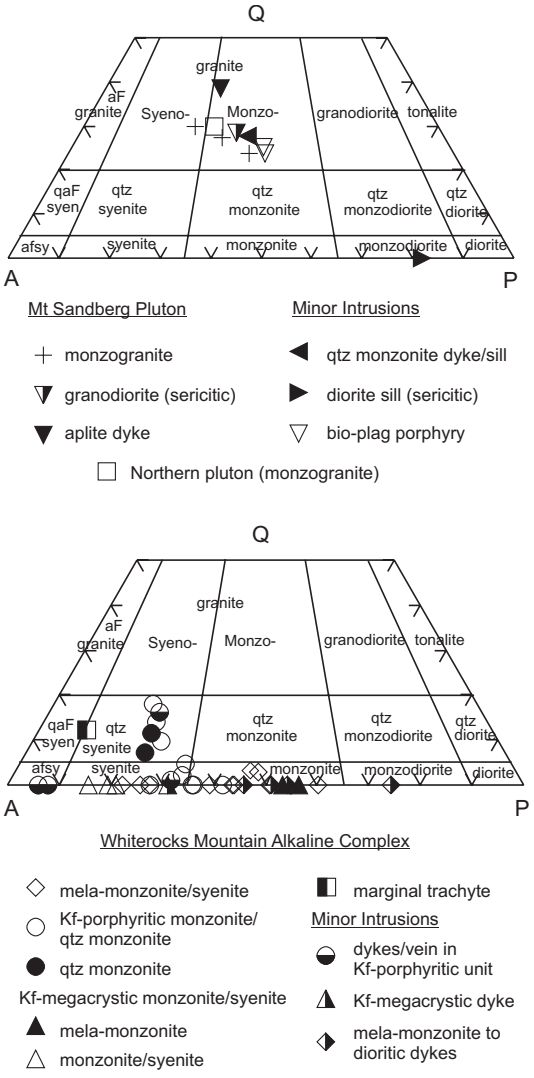

Figure 10. CIPW-normative compositions (wt. %) of plutonic rocks from the Whiterocks complex and other intrusions in the area projected into the QAP classification scheme of Le Maitre *et al.* (1989).

no modal felspathoid minerals are present, the foid-equivalent part of this classification scheme has been ignored. Accordingly, rocks that have normative *ne* (all Kf-megacrystic rocks, practically all mela-monzonites/syenites and the least siliceous Kf-porphyritic rocks of the Whiterocks complex) are forced to plot on the A-P join. This permits a rigourous comparison between modal and normative mineralogy in these feldspathoid-free rocks, particularly with respect to alkali feldspar:plagioclase (A:P) ratios.

As shown in Figure 10, the Whiterocks Mountain alkaline suite is quite distinct from granitoid rocks of the Mt. Sandberg pluton, as well as practically all minor intrusions not associated with the Whiterocks suite, all of which are enriched in normative *qz* at equivalent A:P ratios. The Whiterocks fractionation trend forms a linear array away from the P apex and exhibits a marked bifurcation towards Q-rich and A-rich components for the most differentiated members of the suite (Figure 10). The melanocratic monzonite-syenite rocks extend from alkali-poor monzonite to syenite, and microcline-megacrystic rocks form two distinct groups of monzonites and syenites, all in good agreement with their modal mineralogy. Microcline-porphyritic rocks extend from the monzonite field through syenite to quartz syenite, and together with the non-porphyritic quartz monzonite, are displaced to higher A:P ratios than in the equivalent modal classification scheme. Minor intrusions associated with the Whiterocks aklkaline suite extend the range of rock types from monzodiorite (plagioclase-pophyritic dike) to alkali-feldspar syenite (leuco-syenite dike and a pegmatitic segregation vein), and the marginal trachyte phase lies on the quartz syenite - quartz alkali-feldspar syenite boundary. The displacement of the more differentiated CIPW-normative compositions to higher A:P ratios relative to the modal scheme stems mainly from the inability of the normative calculation to represent important fractionating hydrous minerals (amphibole, biotite) which contain significant amounts of alkalies. A contributing factor may have been a systematic understimation of the modal abundance of potassium feldspar either in the fine-grained groundmasses of minor intrusions or in rocks with a non-uniform distribution of potassium feldspar megacrysts/phenocrysts.

The normative compositions of rocks belonging to the Mt. Sandberg pluton, a granitoid intrusion at the northern edge of the map area and biotite-plagioclase porphyry dikes north of the Whiterocks complex are classified as monzogranites (Figure 10), which is consistent with their mineralogy. The single exception is a biotite-bearing quartz porphyry which falls just within the syenogranite field. Sericitic alteration may account for the monzogranite classification of a granodiorite dike, and likewise, a clinopyroxene-phyric diorite sill which falls within the monzodiorite field.

In an alkalies-silica diagram (Figure 12), the granitoid rocks are distinctly subalkaline except for the monzodiorite sill which is transitional. In an alkalies-iron-magnesia plot (Figure 13), these rocks are calc-alkaline. In contrast (Figure 12), early melanocratic fractionates of the Whiterocks complex together with associated minor intrusions form a differentiation trend within the alkaline field which diverges for more felsic magmas into a pronounced alkaline lineage and a well-defined offshoot which crosses the discriminant boundary into the subalkaline field, and reflects the increasingly *qz*-normative nature of these rocks. The dichotomous bahaviour of these felsic differentiates indicates that more than one fractionation process has governed the evolution of the Whiterocks Mountain alkaline suite. The trend towards subalkaline compositions crosses the low-pressure thermal divide (approximately coincident with the discriminant boundary given in Figure 12) which separates alkaline and subalkaline rock series at pressures below about 5 kb in *anhydrous* systems (Yoder and Tilley, 1962). As discussed previously, the vesicular nature of the marginal trachyte phase implies that, given reasonable volatile concentrations, the Whiterocks alkaline

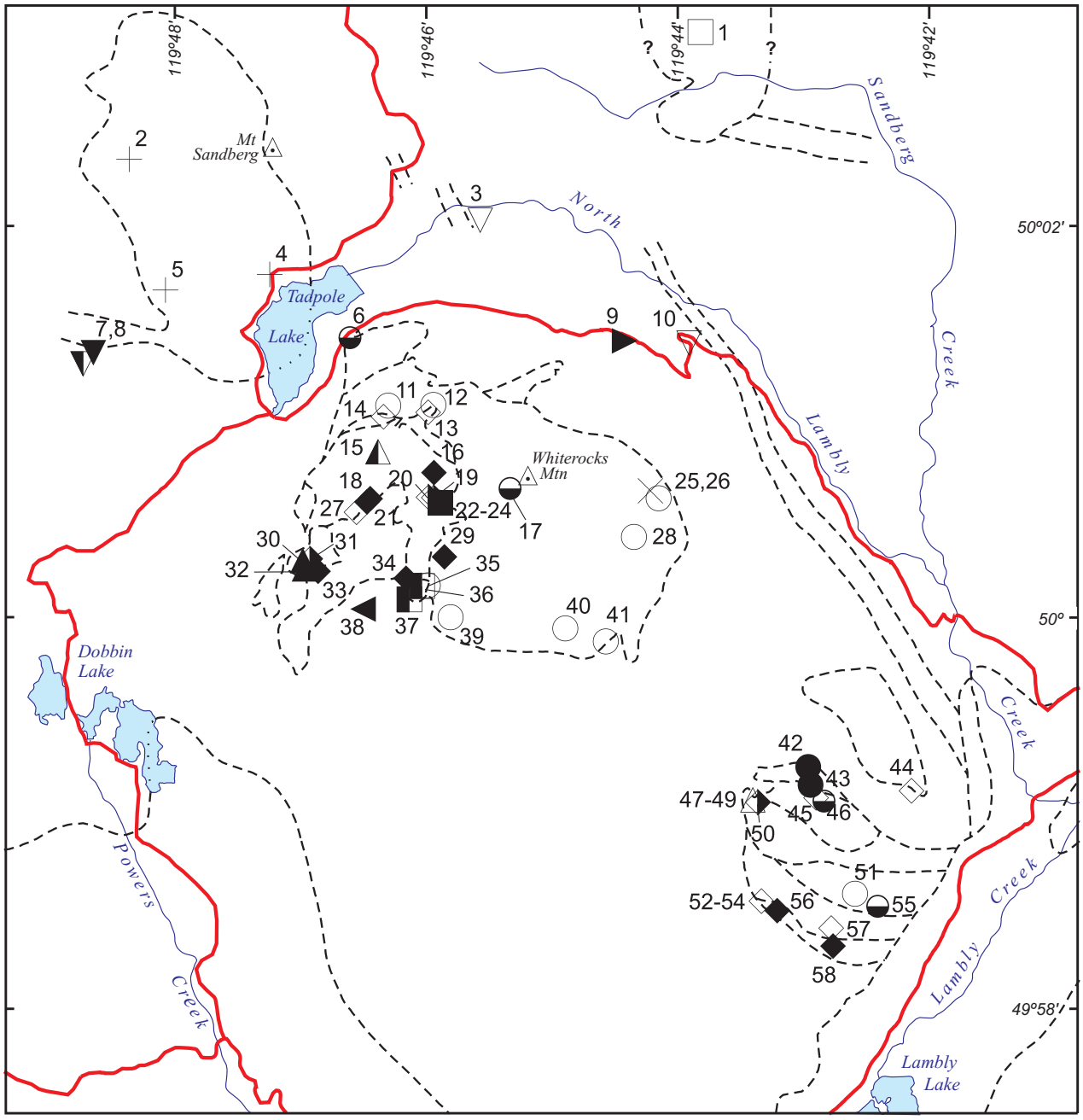

Figure 11. Location of sample sites for whole-rock major element analyses given in Table 6 and plotted in Figure 10. Symbols correspond to those shown in Figure 10 except for a reconstituted xenolith (X).

suite was emplaced at low pressures, probably within several kilometres of the paleosurface. The quartz-normative offshoot from the Whiterocks alkaline trend, therefore, indicates that either the fractionation of hydrous minerals such as biotite and hornblende played an important role in driving these magmas across the thermal divide, or open-system fractionation processes prevailed in the form of crustal contamination of alkaline magmas with *qz*-normative country rocks, or possibly both mechanisms were operating concurrently.

Ultramafic Rocks

The clinopyroxenites and hornblendites are characterized by relatively low alumina (5-10 wt. %) and MgO (7-11 wt. %), moderate TiO_2 (1-1.8 wt. %) and high FeOt (20-25 wt. %), CaO (15-19 wt. %), K_2O (0.5-1.7 wt. %) and P_2O_5 (0.9-1.7 wt. %). Their compositions reflect the accumulation of major silicate liquidus or near-liquidus phases such as high-Ca clinopyroxene, biotite and hornblende, together with accessory phases such as magnetite and apatite. Their relatively low Mg-numbers (100Mg/(0.85Fe+Mg) = 40-61) and cumulate mineral

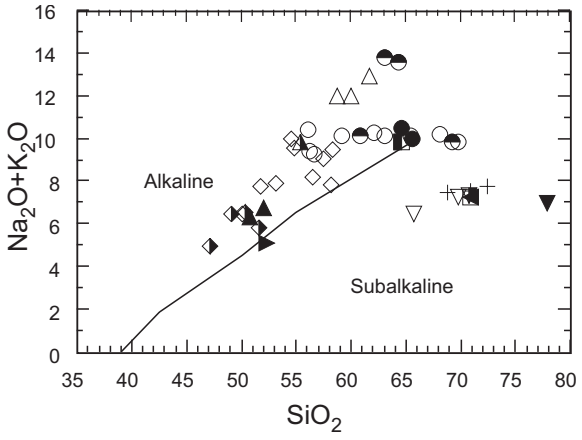

Figure 12. Alkalies versus silica plot (wt. %) for the Whiterocks Mountain alkaline suite and other intrusions within the map area showing the discriminant of Irvine and Baragar (1971) between alkaline and subalkaline fields.

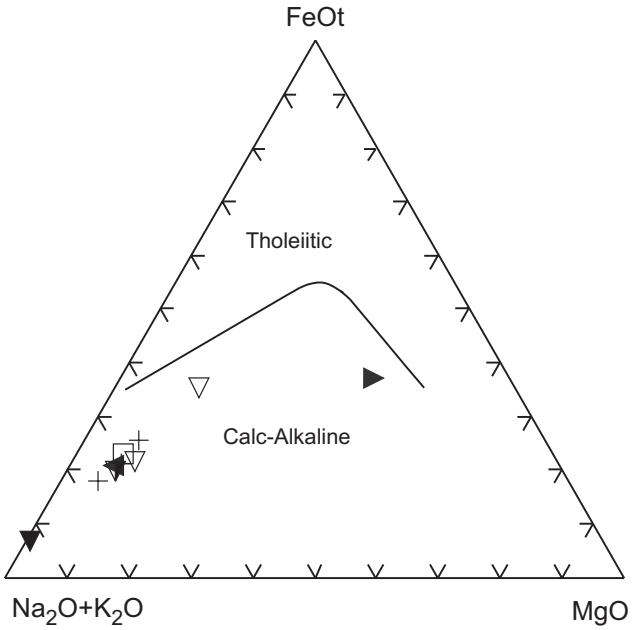

Figure 13. Alkalies-total iron-magnesia plot (wt. %) for calc-alkaline granitoid rocks in the area showing the discriminant of Irvine and Baragar (1971) between the calc-alkaline and tholeiitic fields.

compositions indicate that magmas parental to these ultramafic rocks were not primitive mantle-equilibrated melts but rather evolved, Fe-enriched compositions. In particular, apatite and magnetite are important modal constituents of these rocks (~3-4 and 7-8 vol. %, respectively) and attest to the relatively early saturation of these phases in Fe-enriched, alkaline mafic magmas.. In particular, cumulate apatite is present in anomalous abundances in certain PGE-enriched rocks containing disseminated and partially remobilized sulfides which may be magmatic in origin. The strong positive correlation between P_2O_5 and FeOt in the Whiterocks alkaline suite as a whole indicates that apatite and magnetite were co-crystallizing throughout the entire magmatic evolution (Figure 14).

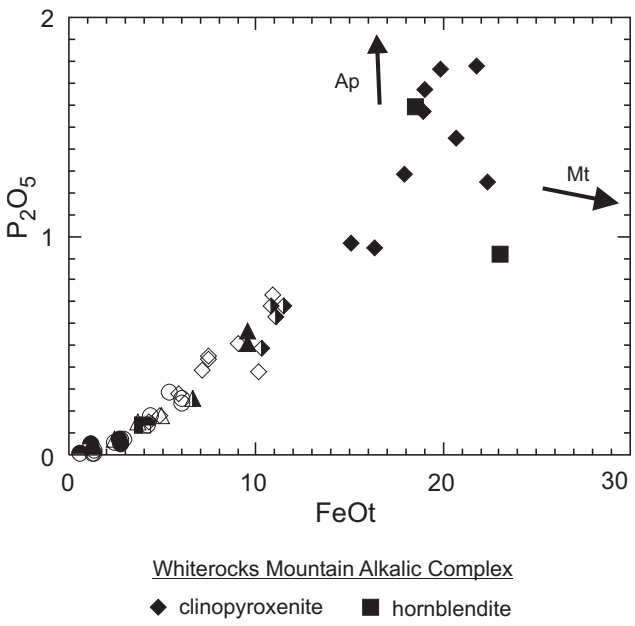

Figure 14. Plot of P_2O_5 versus FeO as total iron (wt. %) for the Whiterocks Mountain alkaline suite showing the high phosphorus and iron contents of clinopyroxenite and hornblendite cumulates. Arrows indicate the effects of accumulation of apatite (Ap) and magnetite (Mt). Symbols for the feldspathic rocks are those of Figure 10.

LITHOGEOCHEMICAL ASSAYS

Mineralized and unmineralized rock samples were prepared using the same crushing and grinding techniques as those employed for the whole-rock samples. Mineralized samples were analyzed by Acme Analytical Laboratories Ltd., Vancouver, for major and minor elements (including sulphur) and a suite of 42 trace elements including base and precious metals and PGE (Pt and Pd). Rock powders (1 g) were digested in aqua regia which is generally expected to yield "near-total" recovery of base and precious metals, and acts as a partial leach for rock-forming (lithophile) elements. Solutions were analyzed by inductively-coupled-plasma mass spectrometry (ICP-MS) and emission spectroscopy. The results are given in Table 7.

A hidden sulfide standard (SU-1a) included in the ICP-MS run (Table 7) yielded base metal concentrations (Ni, Co and Cu) slightly lower than the values recommended by Steger and Bowman (1980). However, the relatively high metal concentrations for Ni and Cu in the standard exceed or lie just below the maximum concentration of the analytical method (10 000 ppm). The results for precious metals (Ag and Au) also appear low, and the PGE show diverse behaviour with Pd in excellent agreement with the standard whereas Pt is anomalously low. It would appear that the acid digest provides "near-total" extraction for base metals, and also Pd in this sulfide-bearing standard, whereas Ag, Pt and possibly Au are problematic. The single duplicate analysis of an unknown shows excellent agreement for all elements except Au.

TABLE 7
LITHOGEOCHEMICAL ANALYSES OF MINERALIZED PLUTONIC AND COUNTRY ROCKS

				wt. %									ppm			
Sample	Depth (ft)	Rock Type	Alteration/Mineralization	Ti	Al	Fe	Mg	Ca	Na	K	P	S	Li	Be	B	Cs
00GNX 3-1-1	outcrop	metasediment	silicified, pyritic, sericitic	0.011	0.29	2.43	0.16	0.04	0.040	0.15	0.033	1.20	6.5	0.3	2	0.57
00GNX 3-17-4	outcrop	aplite dyke	pyritic	0.028	0.48	0.90	0.20	0.21	0.057	0.13	0.027	0.29	4.1	0.2	1	0.75
00GNX 4-9-1	outcrop	metasediment (calc-silicate)	silicified, dissem. S	0.179	0.64	3.92	0.25	0.76	0.099	0.14	0.071	2.39	4.9	0.1	2	0.63
00GNX 5-8-1	outcrop	calc-silicate skarn	trace S	0.147	3.61	4.34	0.60	4.20	0.180	0.29	0.025	2.48	18.9	0.8	4	1.52
00GNX 5-8-2	outcrop	calc-silicate skarn	trace S	0.150	1.07	3.69	0.14	6.00	0.003	0.01	0.017	1.90	1.6	0.1	1	0.18
00GNX 5-8-3	outcrop	calc-silicate skarn	trace S	0.139	0.90	3.42	0.14	4.69	0.005	0.01	0.022	1.72	1.6	0.1	1	0.18
00GNX 8-7-1	outcrop	hornfelsed metasediment	pyritic	0.164	0.63	3.30	0.22	0.88	0.054	0.05	0.119	1.78	9.1	0.5	1	1.2
00GNX 9-9-1	outcrop	Hb monzonite	pyritic	0.115	0.88	2.90	0.18	0.88	0.119	0.07	0.119	1.90	7.3	0.3	1	1.22
00GNX 10-1-1	outcrop	Qz vein	dissem. S	0.049	0.38	1.16	0.30	0.11	0.011	0.24	0.037	0.22	17.9	0.1	1	5.45
00GNX 10-4-2	outcrop	Qz vein	pyritic	0.021	0.27	1.62	0.10	0.61	0.055	0.13	0.010	1.09	13.8	0.1	1	0.85
00GNX 13-5-2	outcrop	Bi cpxite (Ap≤0.5)	dissem. Mt	0.147	0.52	13.46	0.69	0.57	0.023	0.18	0.037	0.02	3.2	0.1	1	0.31
00GNX 16-1-1	outcrop	fBi-Hb cpxite (Ap≤0.3)	dissem. Mt	0.157	2.04	5.87	1.69	3.27	0.292	0.71	0.381	0.04	9.0	0.5	1	0.38
00GNX 16-2-1	outcrop	fCpx hbite (Ap≤0.8)	dissem. Mt	0.180	1.71	9.12	1.24	3.33	0.315	0.43	0.293	0.05	14.2	0.9	1	0.16
00GNX 16-2-5	outcrop	fCpx hbite (Ap≤0.8)	dissem. Mt	0.077	1.74	7.37	1.44	4.13	0.376	0.47	0.632	0.02	6.3	0.6	2	0.17
00GNX 16-2-8	outcrop	Bi-Hb cpxite (Ap≤0.6)	dissem. Mt	0.065	1.75	8.13	1.87	3.02	0.142	1.18	0.621	0.02	24.5	0.1	1	1.44
DDH97-7																
00GNX 30-1	560	fine grained Bi hbite	Mt+Ep veins & patches, Act	0.320	2.23	12.54	2.38	2.23	0.119	1.41	0.349	7.24	18.4	0.3	1	15.03
DDH97-21																
00GNX 53-1	993	fHb cpxite (Ap≤1.3)	Ep+Ser+clay+Act, dissem. S	0.046	1.17	9.76	0.94	4.70	0.170	0.23	0.936	0.27	5.8	0.4	1	0.43
00GNX 53-2	1004	Hb cpxite/Cpx hbite (Ap≤1.3)	Ep+Ab+S veins, Act+Ep, dissem. S	0.086	1.30	9.30	1.11	3.76	0.127	0.45	0.697	5.02	7.5	0.5	1	10.51
00GNX 53-2r	1004	Hb cpxite/Cpx hbite (Ap≤1.3)	Ep+Ab+S veins, Act+Ep, dissem. S	0.086	1.28	9.18	1.09	3.71	0.125	0.45	0.678	4.73	8.1	0.7	2	10.73
00GNX 55-2	1043	Bi-Hb cpxite/Bi-Cpx hbite (Ap≤1.8)	Ep+Cc+S veins, Act	0.088	1.72	9.76	1.64	3.39	0.115	1.05	0.608	3.74	17.8	0.5	2	19.36
00GNX 56-1	1051	fBi-Hb cpxite/fBi-Cpx hbite (Ap≤1.1)	Ep+Cc+S veins, Act, dissem. S	0.081	1.34	8.29	1.17	3.57	0.112	0.64	0.597	2.77	11.9	0.4	2	10.52
00GNX 56-2	1055	fine grained Bi hbite	Ep+Cc veins & patches, Act, dissem. S	0.329	2.37	6.58	2.24	3.51	0.405	0.84	0.179	0.58	20.0	0.4	1	5.04
00GNX 57-1	1070	cpxite	Bi+Act+Ep+S+Mt+Hm veins	0.067	1.33	10.72	1.30	4.43	0.234	0.33	0.653	1.54	7.4	0.8	1	3.89
00GNX 57-2	1075	Hb cpxite/Cpx hbite (Ap≤0.7)	Bi+Act+Ep+S veins & patches, dissem. S	0.092	1.04	6.30	0.92	2.53	0.087	0.43	0.515	2.39	7.0	0.3	2	7.73
00GNX 58-1	1089	Hb cpxite/Cpx hbite	Bi+Ep+Kf+Ms veins & patches, dissem. S	0.439	3.93	7.46	4.27	1.20	0.160	3.37	0.066	0.62	94.6	0.3	2	30.81
00GNX 58-2	1100	Hb cpxite/Cpx hbite (Ap≤0.6)	Ep+Cc+S veins, Act, dissem. S	0.123	0.89	7.99	0.67	2.63	0.116	0.14	0.406	2.05	4.2	0.3	2	0.76
00GNX 60-1	1131	fHb cpxite (Ap≤1.4)	Ep+Cc+S veins, Ep+Ser, dissem. S	0.122	0.75	9.08	0.61	2.90	0.081	0.10	0.389	1.06	4.8	0.3	1	0.47
00GNX 60-2	1137	Hb cpxite (Ap≤0.8)	Act	0.059	0.73	9.19	0.59	3.47	0.089	0.08	0.647	0.40	4.2	0.2	2	0.14
00GNX 61-1	1150	Hb cpxite (Ap≤1.4)	Ep veins, dissem. S	0.127	0.89	7.73	0.78	3.04	0.113	0.23	0.412	1.51	5.0	0.4	2	3.18
00GNX 61-2	1160	Hb cpxite (Ap≤1.3)	Ep veins	0.133	0.84	8.16	0.71	2.74	0.100	0.10	0.348	0.81	4.7	0.3	1	0.23
Std SU1a Rec. Value*				0.106	1.61	14.75	1.16	0.58	0.066	0.51	0.051	6.49	15.2	0.2	2	1.65
Std DS2 Rec. Value**				0.098 0.096	1.83 1.69	3.16 3.07	0.63 0.59	0.57 0.52	0.035 0.029	0.17 0.16	0.102 0.090	0.03 0.03	14.8 14.7	0.6 0.6	3 2	3.05 0.52
RSD %***				3.700	2.90	2.10	2.40	3.80	6.500	5.60	3.200	26.90	3.2	16.0	39	3.8
DTL****				0.001	0.01	0.01	0.01	0.01	0.001	0.01	0.001	0.02	0.1	0.1	1	0.1

TABLE 7 CONTINUED
LITHOGEOCHEMICAL ANALYSES OF MINERALIZED PLUTONIC AND COUNTRY ROCKS

	ppm																				
Sample	Rb	Sr	Ba	Y	Zr	Hf	Nb	Th	U	La	Ce	Mn	Sc	V	Cr	Ni	Co	Cu	Mo	Pb	Zn
00GNX 3-1-1	9.3	20.8	130.8	2.77	20.5	0.53	0.02	2.2	1.9	10.5	14.6	43	3.4	198	35.1	29.1	7.5	17.1	28.6	28.5	40.0
00GNX 3-17-4	6.0	7.4	64.0	3.20	22.4	1.18	0.33	12.4	7.2	6.4	9.8	171	1.2	19	17.1	2.1	2.8	17.7	4.0	3.3	6.9
00GNX 4-9-1	6.2	31.8	23.2	7.06	2.5	0.08	0.27	0.6	0.2	2.5	4.4	104	2.0	45	18.5	17.8	14.1	262.8	26.5	11.3	25.0
00GNX 5-8-1	12.4	123.1	23.3	13.83	7.5	0.22	0.15	0.8	2.3	6.5	8.8	126	3.6	74	29.7	12.4	13.0	63.2	10.6	2.2	36.2
00GNX 5-8-2	0.4	30.9	5.3	27.99	11.2	0.30	0.46	0.6	1.7	9.5	11.2	267	2.3	35	29.8	15.8	12.2	42.0	48.1	3.0	19.9
00GNX 5-8-3	0.4	33.5	8.7	26.07	8.3	0.28	0.49	0.6	1.9	8.3	9.6	195	1.9	29	20.1	11.4	12.5	38.1	25.4	2.0	22.0
00GNX 8-7-1	2.7	20.7	64.9	11.59	5.1	0.21	0.33	2.3	0.6	9.8	17.2	284	3.4	50	15.4	11.1	11.3	119.4	7.9	5.4	55.3
00GNX 9-9-1	2.7	57.1	49.6	7.93	3.9	0.19	0.40	1.8	0.6	8.7	14.5	125	0.8	23	16.4	12.9	10.8	166.2	35.3	3.1	15.3
00GNX 10-1-1	20.1	7.6	48.7	1.70	3.7	0.10	0.15	0.7	0.8	1.0	2.0	213	1.4	37	25.5	9.4	2.7	7.4	5.2	2.3	17.5
00GNX 10-4-2	7.0	30.7	27.9	3.44	1.5	0.05	0.22	1.4	0.4	3.7	6.1	581	0.6	8	17.1	1.2	1.8	2.8	2.7	2.3	9.1
00GNX 13-5-2	7.5	15.2	73.2	1.19	2.5	0.10	0.02	0.1	0.1	0.7	1.7	278	5.9	663	45.0	48.2	45.9	7.1	1.6	1.1	18.8
00GNX 16-1-1	14.7	359.6	431.8	13.29	1.9	0.02	0.02	1.1	0.2	16.2	32.4	841	10.6	251	71.4	25.5	30.2	148.2	0.8	0.9	62.7
00GNX 16-2-1	3.8	200.9	108.9	15.19	3.8	0.04	0.04	1.5	0.3	14.8	30.7	1413	8.5	357	29.8	13.7	26.2	71.3	1.6	5.3	157.3
00GNX 16-2-5	5.2	222.2	113.1	21.67	1.3	0.02	0.02	1.9	0.5	25.2	50.5	1383	10.1	310	17.1	10.2	25.3	182.8	0.5	1.4	94.9
00GNX 16-2-8	49.1	289.9	631.2	19.58	0.4	0.02	0.02	1.4	0.4	23.9	47.6	1038	7.1	369	33.4	18.3	34.9	182.8	1.4	1.5	95.2
DDH97-7																					
00GNX 30-1	65.3	29.3	36.2	8.56	5.0	0.14	0.04	0.3	0.1	2.9	8.6	1014	11.6	320	8.3	41.7	142.0	7068.9	1.2	1.7	97.6
DDH97-21																					
00GNX 53-1	4.4	129.1	37.6	21.32	0.5	0.02	0.02	1.7	0.3	13.8	31.9	842	7.7	675	14.2	23.1	28.2	1938.0	1.0	1.6	81.5
00GNX 53-2	33.5	86.2	24.5	13.01	1.0	0.02	0.02	1.0	0.2	6.2	14.4	730	8.6	348	10.8	21.7	72.7	1385.7	0.9	4.9	79.4
00GNX 53-2r	33.5	85.2	24.2	12.72	1.1	0.02	0.02	1.0	0.2	6.3	15.0	720	8.3	341	12.9	21.6	69.0	1364.1	0.8	5.0	78.0
00GNX 55-2	95.1	73.1	64.6	14.19	0.3	0.02	0.02	0.8	0.2	6.9	16.5	805	7.1	359	16.1	24.3	59.2	1050.0	1.5	4.2	106.6
00GNX 56-1	59.6	108.6	28.7	13.93	0.7	0.02	0.02	0.8	0.2	7.0	16.6	654	5.3	383	12.7	17.4	59.8	452.0	0.9	4.8	63.8
00GNX 56-2	23.7	109.0	135.1	10.07	10.8	0.40	0.02	0.2	0.1	2.6	7.3	902	21.4	370	5.8	20.6	39.5	2360.8	0.5	2.0	72.9
00GNX 57-1	10.6	123.0	42.6	13.43	0.5	0.02	0.02	0.7	0.1	6.1	15.6	920	11.5	546	11.5	24.6	53.7	1475.3	0.9	3.4	83.1
00GNX 57-2	27.2	106.9	56.0	11.41	0.5	0.02	0.02	0.6	0.1	6.1	13.7	485	6.1	254	14.9	27.2	42.5	5535.5	0.8	2.7	160.9
00GNX 58-1	197.3	27.7	426.4	7.77	3.8	0.13	0.02	0.1	0.1	0.8	2.5	946	11.4	326	75.8	57.3	59.4	3588.0	2.5	1.5	125.1
00GNX 58-2	2.6	54.1	14.9	9.69	2.4	0.04	0.02	0.7	0.1	4.6	11.1	499	5.4	361	18.0	47.7	56.8	20481.3	1.0	2.5	178.5
00GNX 60-1	2.6	58.6	12.2	9.15	1.9	0.03	0.03	0.5	0.1	5.3	12.1	528	4.2	600	24.0	33.6	39.1	12254.4	0.5	0.9	137.1
00GNX 60-2	1.2	67.6	9.4	13.07	0.9	0.02	0.02	0.7	0.1	8.8	19.5	523	5.1	659	15.1	30.9	29.6	3911.7	1.0	1.8	98.6
00GNX 61-1	14.1	56.4	12.3	9.79	2.0	0.04	0.03	0.4	0.1	4.4	10.5	561	6.2	458	28.1	22.6	33.4	3849.1	0.7	1.3	102.5
00GNX 61-2	1.7	64.1	19.3	9.08	2.2	0.04	0.02	0.4	0.1	4.8	11.3	519	6.0	568	27.3	26.2	35.0	6233.9	1.1	2.2	113.7
Std SU1a	23.8	21.8	55.2	4.51	2.0	0.08	0.18	3.3	1.8	12.8	26.2	414	1.7	52	141.2	10981.1	331.7	8315.5	1.2	59.9	133.1
Rec. Value*																12330.0	410.0	9670.0			
Std DS2	13.1	28.0	165.7	7.66	3.2	0.03	1.32	3.6	18.9	15.6	30.5	844	3.0	78	172.5	37.2	11.5	130.3	14.5	32.7	163.1
Rec. Value**	12.6	27.7	146.5	7.70	2.9	0.05	1.25	3.7	19.0	15.6	30.0	815	2.9	76	158.4	35.0	11.9	128.0	13.9	32.0	160.0
RSD %***	9.6	4.3	2.7	2.60	7.7	19.50	6.50	4.1	4.9	4.4	3.1	2.2	4.7	2.4	3.2	3.8	3.6	2.1	2.7	3.7	2.5
DTL****	0.1	0.5	0.5	0.10	0.1	0.02	0.02	0.1	0.1	0.5	0.0	1	0.1	2	0.5	0.1	0.1	0.01	0.01	0.01	0.1

TABLE 7 CONTINUED
LITHOGEOCHEMICAL ANALYSES OF MINERALIZED PLUTONIC AND COUNTRY ROCKS

	ppm											ppb					
Sample	As	Sb	Bi	Tl	Ga	Ge	Cd	In	Sn	Se	Te	Re	Hg	Ag	Au	Pt	Pd
00GNX 3-1-1	15.4	1.63	0.55	0.10	1.4	0.1	0.06	0.04	0.3	7.1	0.13	28	9	282	0.4	3	10
00GNX 3-17-4	0.8	0.03	0.28	0.06	2.3	0.1	0.05	0.02	0.3	0.2	0.12	1	5	59	1.1	2	10
00GNX 4-9-1	0.4	0.05	6.86	0.06	2.5	0.1	0.51	0.02	0.6	3.5	0.78	17	5	629	2.0	2	10
00GNX 5-8-1	0.1	0.04	0.22	0.06	7.7	0.1	0.39	0.02	0.4	1.3	0.20	16	5	304	2.2	2	11
00GNX 5-8-2	0.1	0.09	0.15	0.02	2.9	0.1	0.23	0.03	0.7	1.2	0.07	39	5	202	1.1	2	10
00GNX 5-8-3	0.1	0.07	0.18	0.02	2.4	0.1	0.26	0.03	0.4	1.2	0.14	23	5	332	0.8	2	10
00GNX 8-7-1	0.7	0.10	1.75	0.04	2.5	0.2	1.54	0.06	1.1	1.6	0.11	3	6	285	1.4	2	10
00GNX 9-9-1	1.3	0.06	0.54	0.04	2.0	0.1	0.10	0.04	0.4	2.0	0.18	47	5	263	1.2	2	10
00GNX 10-1-1	6.5	0.16	0.17	0.11	2.2	0.1	0.01	0.04	1.6	0.2	0.03	1	5	72	0.5	2	10
00GNX 10-4-2	3.9	0.07	1.18	0.04	1.1	0.1	0.06	0.05	0.3	0.3	0.10	1	5	104	1.3	2	10
00GNX 13-5-2	0.1	0.02	0.02	0.02	7.4	0.1	0.04	0.07	0.7	0.1	0.02	2	6	12	0.8	2	10
00GNX 16-1-1	0.1	0.02	0.02	0.02	6.7	0.2	0.08	0.08	0.7	0.1	0.02	1	5	103	6.6	2	24
00GNX 16-2-1	1.0	3.39	0.10	0.02	8.2	0.2	0.19	0.11	1.4	0.1	0.04	1	6	102	2.4	3	17
00GNX 16-2-5	0.6	0.05	0.02	0.02	7.8	0.2	0.12	0.11	1.1	0.1	0.02	1	5	119	6.6	2	34
00GNX 16-2-8	0.1	0.03	0.02	0.06	9.0	0.2	0.09	0.09	0.8	0.1	0.02	1	6	151	12.1	2	38
DDH97-7																	
00GNX 30-1	0.8	0.04	2.30	0.31	7.0	0.3	0.67	0.14	0.5	7.2	0.31	13	9	2686	72.7	56	77
DDH97-21																	
00GNX 53-1	1.3	0.31	0.54	0.02	7.9	0.2	0.73	0.11	1.0	0.9	0.16	2	7	1163	28.0	299	893
00GNX 53-2	3.2	0.14	3.13	0.21	7.1	0.3	0.71	0.10	1.0	3.5	0.31	1	5	810	75.6	437	375
00GNX 53-2r	3.3	0.14	3.24	0.22	6.8	0.3	0.72	0.10	0.8	3.5	0.32	1	5	815	101.1	443	353
00GNX 55-2	1.5	0.10	2.50	0.56	8.8	0.3	0.95	0.08	0.9	2.6	0.35	1	9	1100	3.3	397	299
00GNX 56-1	2.1	0.11	2.36	0.30	7.0	0.3	0.43	0.08	0.9	1.9	0.16	1	5	434	1.9	295	185
00GNX 56-2	0.1	0.06	0.75	0.11	7.8	0.2	1.63	0.11	1.2	0.8	0.08	1	5	2246	14.1	27	60
00GNX 57-1	13.2	2.99	2.07	0.08	7.3	0.3	1.99	0.09	0.9	1.2	0.52	1	5	1812	1.9	493	882
00GNX 57-2	0.7	0.26	3.19	0.24	5.0	0.2	18.02	0.09	0.7	1.7	1.17	1	9	10148	12.3	1141	1512
00GNX 58-1	0.1	0.04	2.45	0.89	11.5	0.2	2.90	0.07	0.4	1.2	2.20	9	5	4731	9.8	1880	442
00GNX 58-2	1.2	0.20	7.06	0.07	5.0	0.2	5.53	0.14	0.9	10.2	1.56	1	18	22911	83.6	1763	2034
00GNX 60-1	0.9	0.89	1.40	0.02	6.8	0.2	3.37	0.09	0.7	7.5	0.60	1	5	6432	67.3	1790	3018
00GNX 60-2	0.5	0.12	1.07	0.02	7.4	0.1	0.85	0.04	0.8	1.6	0.33	2	6	2546	30.4	1050	585
00GNX 61-1	0.8	0.16	1.31	0.12	6.4	0.2	5.09	0.05	0.8	2.0	0.15	1	5	3523	13.3	271	549
00GNX 61-2	0.6	0.51	1.13	0.02	6.6	0.1	1.39	0.05	0.9	3.0	0.28	1	7	2792	54.2	999	2289
Std SU1a	27.0	2.97	3.86	0.37	5.1	0.3	1.64	0.18	3.7	23.6	1.65	25	5	2852	100.9	134	363
Rec. Value*														4300	150.0	410	370
Std DS2	59.5	9.38	11.22	1.87	6.2	0.1	10.19	5.09	25.1	2.3	1.86	2	235	257	193.9	2	10
Rec. Value**	58.0	9.50	10.92	1.87	6.0	0.0	10.45	5.25	25.2	2.3	1.90	1.5	239	258	208.4		
RSD %***	4.1	3.40	3.50	2.90	3.6	0.0	2.90	6.20	3.5	4.3	3.80	46.9	4.5	3.0	10.0		
DTL****	0.1	0.02	0.02	0.02	0.0	0.1	0.01	0.02	0.0	0.1	0.02	1	5	2	0.2	2	10

Analytical method: 1g sample powder (-150 mesh, W-carbide mill) dissolved in 6 ml HCl-HNO3-H2O (2:2:2) at 95°C and diluted to 20 ml prior to ICP-MS/ES analysis.
Sample locations given in Table A2 (Appendix). "Near-total" leach: Au, Ag, As, Bi, Cd, Co, Cu, Ni, Mo, Pb, Sb, Se, Te, Tl, Zn, Hg, Ge, Re, Sn, Pt, Pd.
Partial loss due to volatilization: As, Sb. Partial leach for remaining elements.
Abbreviations: Hb, hornblende; Bi, biotite; Cpx, calcic clinopyroxene; Qz, quartz; Ap, apatite; Mt, magnetite; Hm, hematite; S, sulphide; Ep, epidote; Ab, albite; Kf, potassium feldspar; Ms, muscovite; Ser, sericite; Act, actinolite-tremolite; f, feldspathic; cpxite, clinopyroxenite; hbite, hornblendite; apatite grain size given in millimetres. r = replicate analysis.
* Steger and Bowman (1980) except Au **In-house standard, Acme Analytical Laboratories *** Relative standard deviation **** Detection limit
ppm, parts per million ppb, parts per billion

TABLE 8
LITHOGEOCHEMICAL ASSAYS FOR PLATINUM-GROUP ELEMENTS
IN DIAMOND DRILL HOLE 97-21, DOBBIN MAIN COPPER ANOMALY

		ppb								g
Sample	Method*	Os	Ir	Ru	Rh	Pt	Pd	Au	Re	Mass
00GNX53-2	INAA	19	1.9	<5	2.6	424	282	63	<5	50
00GNX 53-2	FA				<5	411	321			15
00GNX 53-2	ICP-MS					437	375	76	1	1
00GNX 53-2dup	ICP-MS					443	353	101	1	1
00GNX55-2	INAA	6	0.7	<5	1.4	379	201	4.4	<5	50
00GNX 55-2	FA				<5	397	264			15
00GNX 55-2	ICP-MS					397	299	3	1	1
00GNX 56-1	FA				<5	233	131			15
00GNX 56-1	ICP-MS					295	185	2	1	1
00GNX56-2	INAA	<2	<0.1	<5	0.3	39	40	3.9	<5	50
00GNX 56-2	FA				<5	15	41			15
00GNX 56-2	ICP-MS					27	60	14	1	1
00GNX 57-1	FA				5	628	881			15
00GNX 57-1	ICP-MS					493	882	2	1	1
Standards										
SARM-7	INAA	63	73	430	235	3710	1500	310	<5	10
SARM-7dup	INAA	65	73	420	245	3750	1550	310	<5	10
Rec. Value**		63	74	430	240	3740	1540	310		
INAA DTL		2	0.1	5	0.2	5	2	0.5	5	

		ppb								g
Method*	Sample	Os	Ir	Ru	Rh	Pt	Pd	Au	Re	Mass
INAA	00GNX57-2	15	1.8	<5	4	1150	929	67	<5	50
FA	00GNX 57-2				<5	1185	1647			15
FA	00GNX 57-2dup				<5	1205	1345			15
ICP-MS	00GNX 57-2					1141	1512	12	1	1
FA	00GNX 58-1				<5	1922	353			15
ICP-MS	00GNX 58-1					1880	442		9	1
INAA	00GNX58-2	560	7.3	<5	7	2550	1378	91	<5	50
FA	00GNX 58-2				13	2648	1928			15
ICP-MS	00GNX 58-2					1763	2034	84	1	1
FA	00GNX 60-1				17	3319	2650			15
ICP-MS	00GNX 60-1					1790	3018	67	1	1
FA	00GNX 60-2				5	1789	588			15
ICP-MS	00GNX 60-2					1050	585	30	2	1
	Standards									
FA	FA-10R				103	480	498			15
	Rec. Value***				100	500	500			
	FA DTL				5	1	1			
ICP-MS	SU1a					134	363	101		1
	Rec. Value****					410	370	150		
	ICP-MS DTL					2	10	0.2		

* INAA, Instrumental Neutron Activation Analysis using NiS fire assay preconcentration, Activation Laboratories Ltd., Ancaster, Ontario; FA, fire assay preconcentration using Au inquart and Inductively-coupled plasma (ICP) finish, Acme Analytical Laboratories Ltd., Vancouver; ICP-MS, ICP mass spectrometry and emission spectroscopy analysis using an aqua regia digest, Acme Analytical Laboratories Ltd., Vancouver. ppb, parts per billion dup, duplicate analysis
** Steele *et al.* (1975) *** In-House standard **** Steger and Bowman (1980) except Au DTL, Detection limit

Notwithstanding the reservations outlined above, the results for surface samples reveal some interesting trends. In general, the highest overall abundances of sulphur (1.2-2.5 wt. %), Mo (8-48 ppm), Re (3-47 ppb) and Ag (202-629 ppb), and the highest abundance of Cu (263 ppm), Pb (28 ppm) and As (15 ppm) in any one sample are found in altered sulfide-bearing metasedimentary rocks and calc-silicate skarns near the contacts of the calc-alkaline Mt. Sandberg and northern plutons, and a related monzonitic dike at Tadpole Lake which intrudes the Harper Ranch Group near the northern margin of the alkaline complex. Pt and Pd in all these rocks are near or below detection limits and pyritic quartz veins cutting Whiterocks leucocratic quartz monzonite are metal poor. Interestingly, despite low abundances of sulphur (~200-500 ppm), clinopyroxenites and hornblendites from the northern cupola (*i.e.* excluding biotite clinopyroxenite sample 00GNX-13-5-2 from the southern cupola) have weak but anomalous enrichments in Cu (71-183 ppm), Zn (63-157 ppm), Pd (17-38 ppb) and Au (2.4-12 ppb), and low abundances of Mo and Re, and also have relatively low Ag. It is important to note that these rocks are among the freshest samples collected and seem to be free of hydrothermal veining. Thus, the metal signatures in the surface lithogeochemistry, though subtle, appear to indicate contrasting elemental associations: a Cu-Pd (-Zn±Au) association which appears to be a primary magmatic fingerprint related to ultramafic lithologies of the alkaline complex; and a Mo-Re (-Ag±Cu±Pb±As) association related to the calc-alkaline stocks.

Comparison of Platinum-Group-Element Assays

In addition to ICP-MS analysis, a subset of sulfide-enriched samples from drill core was selected for analysis by fire assay for Pt, Pd and Rh using a 15g sample aliquot and Au inquart (Acme Analytical Laboratories Ltd.), and by neutron activation (Activation Laboratories, Ancaster, Ontario) using nickel sulfide preconcentration for PGE, Re and Au . In particular, hole DDH97-21, which consistently yielded anomalous abundances of Pd (0.41 g/t) and Pt (0.35 g/t) over 111 m, was re-sampled. The analyzed samples represent small widths of core (~10 cm) with relatively abundant disseminated and veins of sulfide in a fairly uniform host (biotite- and hornblende-bearing clinopyroxenite ± feldspar). The analytical results are given in Table 8 and sample locations are listed in the Appendix (Table A2).

It is evident that the various analytical techniques appear to give reasonable reproducibility for Pt and Pd at lower concentrations, but are notably erratic for samples enriched in PGE (>1000 ppb) with three out of five samples yielding anomalously low Pt abundances by acid digestion relative to fire assay. All samples, however, are distinctly enriched in PGE with the highest assays in any one sample (00GNX60-1) reaching 3.3 g/t Pt, 2.6 g/t Pd and 17 ppb Rh. Another sample (00GNX58-2) has highly anomalous Os (560 ppb) and 7 ppb Ir. The abundances of Au are low (<101 ppb) and Re is at or below the detection limit (except 00GNX58-1 with 9 ppb). These results confirm the highly anomalous concentrations of Pt and Pd re-

ported by Verdstone/Molycor from hole DDH97-21 over a substantial width (>100 m) of ultramafic hostrock, and are particularly encouraging with respect to the potential for identifying platinum-group minerals.

MINERALIZATION

Mineralization in the Whiterocks complex occurs in the form of chalcopyrite, magnetite, pyrite, and minor bornite and is primarily hosted by hornblende-bearing clinopyroxenite with scattered sulfide showings in biotite clinopyroxenite and melanocratic monzonite-syenite. As noted previously, the most significant metal-rich area is the "main copper anomaly" near the southwestern margin of the northern cupola (Figure 2).

Mehner (1982) observed that the copper mineralization occurs as both disseminated sulfides and in stringers and fractures associated with epidote and, less commonly, amphibole and minor chlorite. He noted a strong association between magnetite and sulfides in the pyroxenites, and pointed out that grains of magnetite, chalcopyrite and pyrite were commonly found interstitial to clinopyroxene and as inclusions within poikilitic amphibole ("ferrohastingsite") which replaces clinopyroxene. These textural observations, among others, lead Mehner to conclude that the mineralization was related to the intrusion of a sulphur- and copper-enriched "evolved" melt composition which crystallized amphibole (replacing pyroxene), plagioclase, potassium feldspar and sulfides. Sulfide veins and stringers cutting biotite clinopyroxenite and melanocratic monzonite-syenite were related to this intrusive event, which occurred after the crystallization of clinopyroxene but prior to the emplacement of porphyritic monzonite. The conditions under which mineralization occurred were considered to be late magmatic or deuteric and coincident with the crystallization of "ferrohastingsite", hornblende and epidote. It appears that all of these observations have since been reconciled with an alkalic porphyry deposit model (MINFILE 082LSW005; *cf.* Panteleyev, 1995; Osatenko, 1979a).

Origin of the PGE: Hydrothermal or Magmatic?

Evidence for a hydrothermal overprint on the ultramafic and melanocratic feldspathic rocks, at least, is strong. But how does this event bear on the origin of the Cu-PGE mineralization?

There are abundant hydrothermal veins and stringers containing pyrite and lesser chalcopyrite±bornite in drill core recovered from the central copper anomaly (Kikauka, 1997). Our own observations in clinopyroxenites and feldspathic hornblendites in core from DDH97-21 have noted sulfide-bearing veins locally associated with epidote, carbonate, quartz, potassium feldspar, biotite, sericite, chlorite, magnetite, and rare hematite and garnet; and Kikauka (*ibid.*) also noticed rare traces of molybdenite in minor shear zones. Most of the vein-hosted sulfides appear to be preferentially associated with epidote, and some of the thicker veins contain a sulfide-rich core surrounded by euhedral epidote at their margins. In addition, geochemical aspects of this hydrothermal signature in the soils over this zone include interelement correlations among Cs, Cu, Mo and Ag (Dunn *et al.* this volume). Interestingly, this signature is very similar to the Mo-Re (-Ag±Cu±Pb±As) signature of hydrothermal systems related to the calc-alkaline stocks in the area, especially the Mt. Sandberg porphyry Mo prospect at Tadpole Lake. The implication is that hydrothermal alteration at the main Dobbin copper anomaly is genetically related to a *calc-alkaline* rather than an alkaline magmatic source.

Despite the strong evidence for hydrothermal alteration, certain aspects of the mineralization are not well explained by purely considering such an origin, not the least of which is the tenor of the PGE over such a large interval (>100m) in DDH97-21, for example, and the close association between sulfides and ultramafic lithologies. On this point, it appears possible to reconcile many of Mehner's observations, and our new results, with a magmatic origin for the Cu-PGE-bearing sulfides, albeit remobilized to variable extents by subsequent hydrothermal activity.

We have a different view of the origin of the hornblende clinopyroxenite which appears to be the most important host for the Cu-PGE mineralization. The evolution of the alkaline magma chamber progressed from the crystallization of clinopyroxene cumulates through hornblende-rich feldspathic cumulates to melanocratic monzonites. Because of the intercalated nature of these lithologies, at least locally, evolution of the magma chamber was evidently punctuated by fresh incursions of more primitive parental magma. The large poikilitic crystals of hornblende in this rock were formed by adcumulus growth of amphibole as calcic clinopyroxene reacted with the liquid at *high* (magmatic) temperatures. Textural evidence for the latter reaction includes the subhedral to rounded and resorbed habit of cumulus pyroxene and the patchy to vermicular replacement by amphibole. Furthermore, it is this reaction that is ultimately responsible for the elimination of clinopyroxene (except as a relict phase) in the more differentiated rocks. Cumulus hornblende crystallized in the melt prior to the disappearance of clinopyroxene and formed the minor hornblendite and hornblende gabbro/diorite lithologies encountered near the clinopyroxenite – melanocratic monzonite transition. Accessory phases such as apatite and magnetite attain their maximum grain sizes and modal abundances in hornblende clinopyroxenites and clinopyroxene hornblendites, and occur as both cumulus and intercumulus minerals; whereas plagioclase in feldspathic variants is only observed as an intercumulus phase and is considered to represent crystallization of trapped residual melt. Both magnetite and apatite are intimately associated with Cu-PGE mineralization in DDH97-21.

As originally described by Mehner (1982), disseminated Cu-PGE sulfides in the clinopyroxenites are commonly enclosed by hornblende and also occur as interstitial grains accompanied by magnetite and apatite. Although not conclusive, such textures are consistent with those commonly attributed to sulfide immiscibility in silicate melts. If one accepts the textural evidence as indicative of a magmatic heritage, an explanation is required for the composition of the sulfides, which are copper-rich as opposed to nickeliferous. In this regard, the most important control on sulfide composition at the onset of immiscibility is the composition of the coexisting silicate melt.

Although accumulative in origin, the pyroxenites are depleted in MgO, as well as Ni and Cr (Table 6 and Mehner, 1982), and, therefore, crystallized from a fractionated mafic parental melt already depleted in these highly compatible elements. The fact that Ni is compatible in early crystallizing silicate minerals and Cu is relatively incompatible has been a fundamental tenet of modern interpretation in igneous petrology. The behaviour of PGE with respect to mafic silicates has been controversial, but interpretations do exist which indicate that Pd is also incompatible in early crystallizing silicates (*e.g.* Barnes and Naldrett, 1986). Thus, a magma evolving by crystal fractionation would be expected to concentrate Cu, and potentially Pd, in mafic residual liquids up to the point of sulfide immiscibility. Since Whiterocks clinopyroxenites are the predominant host of disseminated sulfides and have the highest copper abundances (6-357 and averaging 142 ppm Cu for biotite clinopyroxenites; 129-5550 ppm and averaging 853 ppm Cu in hornblende clinopyroxenites; Mehner, 1982), melts that crystallized the clinopyroxenites must also have achieved sulfide saturation.

It is also possible to explain the tenor of PGE in these sulfides by appealing to igneous processes of the type which were evidently operating in these alkaline magma chambers. Given the evidence cited above for magma chamber replenishment early in the evolution of the alkaline suite, and the widespread indications of convective activity in the form of igneous laminations, including rare examples in the pyroxenites where recognition of such textures usually requires thin-section examination, it is evident that the Whiterocks alkaline rocks evolved in dynamic magma chambers. Under these conditions, small amounts of immiscible sulfide droplets would have been well distributed throughout the magma chamber and exposed to many times their own mass of silicate melt, and in addition, would have come into contact with new batches of metal-enriched, more primitive magma. Such an environment would have been conducive for increasing the tenor of PGE in the sulfide droplets, especially the anomalous abundances of Pt which accompany Pd, given the extremely high partitioning of PGE into sulfide melts.

In conclusion, it is emphasized here that the inferences given above regarding a magmatic origin for Cu-PGE mineralization in the Whiterocks alkaline complex represent a working hypothesis only. Whether or not in fact PGE enrichment actually relates to such an origin remains to be adequately tested by detailed study of the textures and compositions of coexisting oxides, sulfides and silicates, as well as any platinum-group minerals that may be present. If a magmatic heritage for the Cu-PGE association is ultimately considered more likely than a purely hydrothermal origin, there are important implications not only for local controls on mineralization (*i.e.* lithologic and potentially stratigraphic rather than structural) but also for similar base-metal - PGE associations in other alkaline complexes in British Columbia and elsewhere.

ACKNOWLEDGMENTS

We would like to extend our appreciation to the directors of Verdstone Gold Corporation and Molycor Gold Corporation, in particular John Fisher, Larry Reaugh and John Chapman, for freely sharing information on the geology of the Whiterocks complex and allowing us to sample drill core. Sincere thanks to Andris Kikauka for providing geological data and samples of drill core, and for many discussions concerning the Dobbin property. Dave Lefebure and Colin Dunn are thanked for their interest and field visits, and Dave Lefebure for his constructive and timely review of the manuscript.

REFERENCES

Abbey, S. (1979): Reference materials – rock samples SY-2, SY-3, MRG-1; *CANMET* Report 79-35, 66 pages.

Naldrett, A.J. and Barnes, S..J. (1986): The behaviour of platinum-group-elements during fractional crystallization and partial melting with special reference to the composition of magmatic sulfide ores; *Fortschritte der Mineralogie*, Volume 64, pages 113-133.

Cairnes, C. E. (1940): Kettle River (west half) map sheet; *Geological Survey of Canada,* Map 538A.

Geological Survey of Canada (1968): Aeromagnetic map of Shorts Creek, British Columbia; *Geological Survey of Canada,* Map 5207G.

Hulbert, L.J. Duke, M.J., Eckstrand, O.R., Lydon, J.W. Scoates, R.F.J., Cabri, L.J. and Irvine, T.N. (1988): Geological environments of the platinum-group elements; *Geological Association of Canada*, Cordilleran Section Workshop, Vancouver, 151 pages.

Jones, A. G., (1959): Vernon map area, British Columbia; *Geological Survey of Canada*, Memoir 296, 186 pages.

Kikauka, A. (1997): Geological, geochemical and diamond drilling report on the Dobbin claim group, Whiterocks Mountain, Kelowna, B.C; *British Columbia Ministry of Energy and Mines*, Assessment Report 25290.

Knowles, C. R. (1987): A basic program to recast garnet end-members; *Computers and Geosciences*, Volume 13, pages 655-658.

Leake B.E., Woolley, A.R., Arps, C.E.S., Birch, W.D., Gilbert, M.C., Grice, J.D.,Hawthorne, F.C., Kato, A., Kisch, H.J., Krivovichev, V.G., Linthout, K., Laird, J., Mandarino, J.A., Maresch, W.V., Nickel, E.H., Schumacher, J.C., Smith, D.C., Stephenson, N.C.N., Ungaretti, L., Whittaker, E.J.W., and Youzhi, G. (1997): Nomenclature of amphiboles: report of the subcommittee on amphiboles of the International Mineralogical Association, Commission on New Minerals

and Mineral Names; *Canadian Mineralogist*, Volume 35, pages 219-246.

Little, H. W. (1961): Kettle River, west half map area; *Geological Survey of Canada*, Map 15-1961.

Makepeace, D. K. (2000): Summary review of the Dobbin property, Tadpole Lake area, Vernon and Nicola Mining Divisions, British Columbia, Canada; Internal Report for Verdstone/Molycor Gold Corporations, Surrey, British Columbia, 48 pages.

Mehner, D. T. (1982): Geology of the Whiterocks Mountain alkalic complex, South-central British Columbia; unpublished M.Sc. thesis, *University of Manitoba*, 89 pages.

Morimoto, N. (1989): Nomenclature of pyroxenes; *Canadian Mineralogist*, Volume 27, pages 143-156.

Nixon, G.T. Hammack, J.L., Ash., C.H., Cabri, L.J., Case, G., Connelly, J.N. Heaman, L.M., Laflamme, J.H.G., Nuttall, C., Paterson, W.P.E. And Wong, R.H. (1997): Geology and platinum- group-element mineralization of Alaskan-type ultramafic-mafic complexes in British Columbia; *Ministry of Energy and Mines*, Bulletin 93, 142 pages.

Okulitch, A.V. (1979): Geology and mineral occurrences of the Thompson-Shushwap-Okanagan region, south-central British Columbia.

Okulitch, A.V. (1989): Revised stratigraphy and structure in the Thompson-Shuswap-Okanagan map area, southern British Columbia; *Geological Survey of Canada*, Paper 89-1E, pages 51–60.

Osatenko, M.J. (1978): Geological; stream silt, rock and soil geochemical and ground magnetics work on the Dobbin property (Tad 1-6); *British Columbia Ministry of Energy and Mines*, Assessment Report 6732.

Osatenko, M.J. (1979a): Geological; ground magnetics, I.P.; rock and silt geochemical and percussion drilling work on the Dobbin property (Tad 1-6); *British Columbia Ministry of Energy and Mines*, Assessment Report 7269-1.

Osatenko, M.J. (1979b): Assessment report of geology, soil geochemisty, percussion and diamond drilling on the Dobbin property (Tad 1-3, Tad 5-12, Tad 14, Tad 19 and Esperon 11 claims), Tadpole Lake, Vernon and Nicola M. D.*; British Columbia Ministry of Energy and Mines*, Assessment Report 7596.

Osatenko, M.J. (1980): Assessment Report of Percussion Drilling on the Dobbin Property (Tad 1-12, Tad 14, Tad 19-22 claims), Tadpole Lake Area, Vernon and Nicola M. D., B.C.; *British Columbia Ministry of Energy and Mines*, Assessment Report 8456.

Panteleyev, A. (1995): Porphyry Cu-Au alkalic (L03); in Selected British Columbia Mineral Deposit Profiles Volume 1 – Metallics and Coal, Lefebure, D.V. and Ray, G.E., editors, *B.C. Ministry of Energy and Mines*, Paper 1995-20, pages 83-86.

Robinson, P., Spear, F.S., Schumacher, J.C., Laird, J., Klein, C., Evans, B.W. and Doolan, B.L. (1981): Phase relations of metamorphic amphiboles: natural occurrence and theory; *Mineralogical Society of America* Reviews in Mineralogy, Volume 9B, pages 1-228.

Steger, H.F. and Bowman, W.S. (1980): SU1a: a certified nickel-copper-cobalt reference ore; *CANMET* Report 80-9E, 25 pages.

Steele, T.W. (1975): Preparation and certification of a reference sample of a precious metal ore; *National Institute for Metallurgy* (South Africa), Report 1696-1975, 50 pages.

Weeks, R.M., Bradburn, R.G., Flintoff, B.C., Harris, G.R. and Malcolm, G. (1995): The Brenda Mine: the life of a low-cost porphyry copper-molybdenum producer (1970-1990), southern British Columbia; *in* Porphyry Copper Deposits of the Canadian Cordillera*, Canadian Institute of Mining* Special Volume 46, pages 192-200.

Wilkins, A.L. (1981): K-Ar and Rb-Sr dating of the Whiterocks Mountain alkalic complex in the Intermontane Belt west of Okanagan Lake, south-central British Columbia; unpublished B.Sc. thesis, *The University of British Columbia*.

Yoder, H.S. and Tilley, C.E. (1962): Origin of basaltic magmas: an experimental study of natural and synthetic rock systems; *Journal of Petrology*, Volume 3, pages 342-532.

APPENDIX TABLE A1
WITHIN-RUN ELECTRON-MICROPROBE ANALYSES OF INTERNATIONAL STANDARDS

	Diopside			Albite		
Oxide (wt%)	s439nom (accepted)	s439 avg (measured)	% rel dev (2σ)	s430nom (accepted)	s430avg (measured)	% rel dev (2σ)
Na_2O	0.38	0.39	19.56	11.46	11.43	3.743
MgO	17.94	17.83	2.36	-	-	-
Al_2O_3	0.43	0.6	12.07	19.77	19.69	1.814
SiO_2	55.19	55.32	1.33	68.14	69.11	1.224
K_2O	-	-	-	0.23	0.12	51.999
CaO	25.18	25.38	2.64	0.38	0.08	76.64
TiO_2	0.03	0.03	-	-	-	-
Cr_2O_3		0.05	-	-	-	-
MnO	0.06	0.06	-	-	-	-
FeO	0.89	0.86	21.65	0.01	0.01	-
BaO	-	-	-	-	-	-
Total	100.10	100.49		99.99	100.43	

	Orthoclase			Anorthite		
Oxide (wt%)	s438nom (accepted)	s438avg (measured)	% rel dev (2σ)	t101nom (accepted)	t101avg (measured)	% rel dev (2σ)
Na_2O	0.91	0.95	10.929	0.03	0.07	77.477
MgO	-	0.01	-	-	-	-
Al_2O_3	16.74	16.36	1.907	36.5	36.49	1.494
SiO_2	64.8	65.24	1.227	43.3	43.62	1.406
K_2O	15.49	15.44	3.468	-	0.01	-
CaO	-	-	-	20.3	20.25	2.952
TiO_2	-	-	-	-	-	-
Cr_2O_3	-	-	-	-	-	-
MnO	-	-	-	-	-	-
FeO	2.01	1.96	13.519		0.05	-
BaO	0.05	-	-	-	-	-
Total	100.00	99.96		100.13	100.48	

s439 natural diopside standard; s430 natural albite standard; and s438 natural orthoclase standard all supplied by C.M. Taylor Company, Amelia, Virginia, U.S.A.
t101 synthetic anorthite standard, Jun Ito (pure $CaAl_2Si_2O_8$)

APPENDIX TABLE A2
SAMPLE LOCATIONS FOR ICP-MS ANALYSES

	NAD 1983	
Sample	Easting	Northing
00GNX 3-1-1	299477	5544098
00GNX 3-17-4	298672	5544979
00GNX 4-9-1	300417	5547915
00GNX 5-8-1	304359	5547277
00GNX 5-8-2	304360	5547275
00GNX 5-8-3	304360	5547276
00GNX 8-7-1	300802	5545658
00GNX 9-9-1	301170	5545058
00GNX 10-1-1	302714	5542409
00GNX 10-4-2	303773	5543018
00GNX 13-5-2	305525	5539076
00GNX 16-1-1	301897	5543695
00GNX 16-2-1	301945	5543412
00GNX 16-2-5	301945	5543412
00GNX 16-2-8	301945	5543412

	NAD 1983	
Sample	Easting	Northing
DDH97-7		
00GNX 30-1	300773	5542803
DDH97-21		
00GNX 53-1	300762	5542803
00GNX 53-2	300762	5542803
00GNX 53-2r	300762	5542803
00GNX 55-2	300762	5542803
00GNX 56-1	300762	5542803
00GNX 56-2	300762	5542803
00GNX 57-1	300762	5542803
00GNX 57-2	300762	5542803
00GNX 58-1	300762	5542803
00GNX 58-2	300762	5542803
00GNX 60-1	300762	5542803
00GNX 60-2	300762	5542803
00GNX 61-1	300762	5542803
00GNX 61-2	300762	5542803